Revealing the effect of an industrial flash flood on vegetation area: A case study of Khusheh Mehr in Maragheh-Bonab Plain, Iran

Mehrnoosh Taherizadeh [a*], Javid Hojabri Khushemehr[b], Arman Niknam [c], Thong Nguyen-Huy[d,e], Gabor Mezosi[f]

[a] *Department of Geoinformatics physical and Environmental Geography, University of Szeged, Szeged, Hungary*

[b] *Department of Remote sensing and GIS, University of Tehran, Tehran, Iran*

[c] *Department of Geoinformatics physical and Environmental Geography, University of Szeged, Szeged, Hungary*

[d] *Centre for Applied Climate Sciences, University of Southern Queensland, Toowoomba, QLD, Australia*

[e] *Ho Chi Minh City Space Technology Application Center, Vietnam National Space Center, Ho Chi Minh City, Vietnam*

[f] *Department of Geoinformatics physical and Environmental Geography, University of Szeged, Szeged, Hungary*

ABSTRACT

Floods are one of the most significant environmental hazards that can have harmful effects on agricultural activities and vegetation. The primary objective of this study is to analyze the destructive after-effects of an industrial flash flood on the vegetation of the Khusheh Mehr region. This flash flood occurred due to a break in the wastewater ponds of the Kaveh Soda factory on April 25, 2010. Using the Normalized Difference Water Index (NDWI) and the Normalized Difference Vegetation Index (NDVI) derived from time-series Landsat data over the period of 2000-2020, we analyzed the changes in wastewater ponds and regional vegetation before and after the wastewater flood occurred. We also investigate the quantitative and qualitative changes in vegetation during the past 20 years and detect the flood passage through this area. The results show that 538 hectares out of the total 2123 hectares of Khusheh Mehr were directly affected by the runoff resulting from the 2010 flood, and 1250000 m3 of industrial wastewater was discharged in the study area. The analysis of the vegetation in 2010 showed that during May and July, the efficiency and expansion of vegetation in these areas (NDVI > 0.3) decreased by 90% and 55%, respectively, compared to the same periods in 2009 and 2006. The study is significant because it can help evaluate the effects of the flash flood not only on wastewater ponds and vegetation but also on the contamination of underground and surface waters as chemicals and industrial wastewater held in natural and artificial environments are discharged during a flood and directly

Mehrnooshtahereezadeh@gmail.com

affect vegetation. The findings can provide useful information for hazard and land use management and support policymakers, e.g., payment for financial loss of farmers.

Keywords: Flood, Wastewater, Landsat, Khusheh Mehr area, NDVI, NDWI.

1. INTRODUCTION

Floods are considered a tragedy caused by both humans and nature. This catastrophe has occurred most frequently in arid regions in the past decade (Avand et al., 2022) and has caused enormous damage to constructions, infrastructure, land, and fatalities. During the past century, this damage has amounted to up to 386 billion USD (Wang et al., 2011). Between 1995 and 2015, 47% of hazardous accidents with natural origins could be related to floods, affecting the lives of 2.3 billion people globally (Walstorm and Guha-Sapir, 2015).

Floods can generally be categorized into two types: "riverine" and "flash". The former is predictable and has roots in melting glaciers and harsh weather conditions, leaving enough time for management. However, this is not the case for flash floods, which develop quickly in a short period of time (Ritter et al., 2020). Heavy rain, breaks in dams or levees, and seasonal ice jams on rivers during winter and spring are common causes of flash floods (Azam et al., 2017).

When damage to dams and dikes results in flash floods, vegetation, forests, orchards, grazing lands, and farms are considerably affected, turning floods into an environmental threat for plants (Pucciariello et al., 2014). In fact, floods impact 27% of agriculture worldwide (Pasley et al., 2020) by causing damage to plants and limiting the growth of biomass (Pires et al., 2018; Xu et al., 2015). Therefore, the amount of biomass and production falls (Pires et al., 2018; Pucciariello et al., 2014; Watson et al., 1976).

Chemicals and industrial wastewater are typically stored in both natural and man-made environments and are at risk of being discharged during floods (World Meteorological Organization, 2015). Wastewater from factories, which can be either acidic or alkaline, poses significant dangers to aquatic life (Wu, 2017). Hazards that threaten the environment are a contentious issue worldwide, with the potential threats of effluents being particularly concerning. Sewage water contains a significant amount of different pollutants, the most common of which are those that are harmful to both human and natural life, including toxic organic and inorganic substances such as salt, heavy metals, nitrates, and pathogens (Jaramillo and Restrepo, 2017; Khan

Mehrnooshtahereezadeh@gmail.com

and Ali, 2017). It is widely believed that releasing effluents into open spaces can lead to various types of contamination (Youssef et al., 2011), with soil and vegetation deterioration being one of the dangerous outcomes of sewage discharge into the environment (Ali et al., 2014).

Estimating the flooded area and calculating the damage are vital factors in managing flood crises (Long et al., 2014; Shrestha et al., 2021). Many studies have focused on flood preparedness, warning, monitoring, severity, and extent of damage (Ahmed and Akter, 2017; Anusha and Bharathi, 2020; Arvind et al., 2016; Bourenane et al., 2018; Lopes et al., 2019; Marchi et al., 2010; Moharrami et al., 2021; Yariyan et al., 2020).

Remote sensing is one of the most widely used research methods for post-flood change detection (Gandhi et al., 2015). Space-borne sensors provide images of the Earth's surface with adequate spatial and temporal resolution for environmental investigations (Roy et al., 2017). Analyzing multi-temporal time series of satellite images is critical in distinguishing or discriminating between changes in land cover over different periods. New equipment has been introduced for series analysis of changes in the same location (Nusrath, 2010; Arvind et al., 2016).

Remote sensing is described as the art and science of collecting data and extracting information about objects, areas, or phenomena such as vegetation, land cover classification, dew estimation, urban green areas, agricultural land, and water resources, without physical contact (Gandhi et al., 2015; Morar et al., 2022; Valjarević et al., 2020; Verpoorter et al., 2012). Digital processing of images is an effective method to apply various algorithms and mathematical indices to study these features. The specifications are reflectance-based, and indices highlight the areas of interest on the image (Deep and Saklani, 2014). Spectral indices such as Normalized Difference Vegetation Index (NDVI) and Normalized Difference Water Index (NDWI) are widely used and approved for trend analysis in vegetation and surface water covers under temporal resolution (Bhandari et al., 2012; Chen et al., 2013; Rouse et al., 1974). NDVI, calculated as a ratio difference between measured canopy reflectance in the red and near-infrared bands, is particularly helpful in assessing greenery density (C. Tucker, 1979; Vrieling et al., 2013; Rouse et al., 1974; Nageswara Rao et al., 2005; Zhu et al., 2013). To study changes in land cover through indexing the greenness of the land surface and changes in the presence of water bodies on the land surface, NDVI and NDWI were used, respectively (Gao, 1996; Rouse et al., 1974).

Mehrnooshtahereezadeh@gmail.com

It has been repeatedly reported that NDVI can be used for vegetation observations and NDWI for water bodies (Ahmed and Akter, 2017; Ashok et al., 2021; Choubin et al., 2019; Gandhi et al., 2015; Hu et al., 2018; Potter, 2021; Viana et al., 2019) as well as in other studies (Chen et al., 2021; Chouari, 2021; Demirel et al., 2010; Boori et al., 2020; Zhang et al., 2009). The NDWI index has also been widely applied for change detection (Ashok et al., 2021; El-Asmar et al., 2013; Jaramillo and Restrepo, 2017; Saravanan et al., 2019; Viana et al., 2019) and flood studies (Lopes et al., 2019; Memon et al., 2015).

Kaveh-Soda is one of the major factories in Maragheh-Bonab Plain, Azerbaijan Province, Iran, producing sodium carbonate. As a result, the industrial wastewater from this establishment is held in enormous ponds, five of which were breached on April 25, 2010, due to heavy seasonal rainfall (Shahbazi et al., 2015). The resulting flood destroyed all the gardens and agricultural lands in Khusheh Mehr, YengiKand, Narjabad, and Khaneqah, the four downstream villages from the Kaveh Soda factory and wastewater ponds.

Therefore, our study focuses on investigating the effects of the 2010 flood on vegetation in the Khusheh Mehr area and Maragheh-Bonab Plain in Azerbaijan Province, Iran. To accomplish this, we utilize two remotely sensed indicators, NDVI and NDWI, to achieve the following objectives: i) to examine both quantitative and qualitative changes in vegetation in the region during the past 20 years; ii) to assess the changes in area and volume of wastewater ponds before and after the flood; iii) to evaluate the impact of the flood on vegetation in the area; and iv) to detect the path of the flood through the Khusheh Mehr area.

2. FLOOD EVENT AND STUDY AREA

The Maragheh-Bonab Plain is located in the East Azerbaijan province in the northwest of Iran (see Figure 1). Generally, this area experiences a cold and dry climate (Fijani et al., 2017), with an average annual temperature of around 13.5°C, ranging from a minimum of -0.3°C to a maximum of 28.4°C. Annual rainfall levels in the plain range from 306.5 mm to 413.5 mm in the mountainous areas, with most rainfall occurring between March and May. The annual evaporation rate is approximately 1600 mm (Fijani et al., 2013).

Mehrnooshtahereezadeh@gmail.com

Most of the Maragheh-Bonab Plain is covered in alluvial sediments that are between 20 and 80 meters thick (Barzegar et al., 2017). From a hydrogeological perspective, the region's hydrous formations consist of Quaternary sediments that cover most of the plain. These sediments have formed alluvial and free aquifers with good discharge, including river sediments, debris sediments, and high alluvial terraces. Permian calcareous formations in the north of the region, which mainly form the heights, also have good discharge (Asghari Moghaddam et al., 2015). The Sufi Chay river, which originates from the Southern amplitude of Mount Sahand (shown in Figure 5), is the main river in the area. The river flows south-west and enters the city of Maragheh before redirecting to the west and crossing the agricultural lands of Bonab and Khusheh Mehr locality, ultimately emptying into Lake Urmia (Fijani et al., 2017).

Most of the underground water in the Maragheh-Bonab Plain is used for agriculture, with drinking and industrial usage as the second and third priorities (Fijani et al., 2017). The villages in the area benefit from soft, fertile soil, and farming, horticulture, and animal husbandry are the main occupations of the local people (Hamzehpour and Rahmati, 2017). Grape fields, plum, apple, and walnut orchards are well-known in the region, and onions, tomatoes, potatoes, corn, wheat, and barley are also cultivated in this field (Narimani et al., 2011). The flooded area of Khusheh Mehr, including the rural areas of Yengikand, Narjabad, and Khaneqah, covers approximately 2123 hectares with a population of 6657 according to the annual census of 2016 (Statistical Center of Iran, 2016).

The Kaveh Soda factory, situated on the eastern side of the studied area, has been actively producing sodium carbonate (Na2CO3) since 2004. The factory specializes in producing industrial salts, detergents, light and heavy sodium carbonate, baking soda (NaHCO3), and glassware. Sodium carbonate is a substance that is widely used in the paper industry. Consequently, sodium carbonate, with a mass weight of 106 grams, is a white crystalline powder that is the most critical use in the glass industry. Also, the names of soda1 and soda ash2 brands are used for their solid-state (Wang and Wang, 2009). The salt required for the factory is supplied from Lake Urmia. Ammonia is using a considerable amount of freshwater, and a significant volume of ammonia and salts also flow into the environment. It is introduced into the production process but is not consumed, and only a small amount of it is lost. The general reaction to the process follows the

Mehrnooshtahereezadeh@gmail.com

formulas occurring in this factory (Han et al., 2021; Wang and Wang, 2009), and these elements and materials can also be found in the wastewater of Kaveh Soda factory.

The production of one ton of sodium carbonate produces approximately ten cubic meters of effluent, including one ton of calcium chloride, half a ton of sodium chloride, and other soluble and insoluble impurities. Currently, the production unit covers an area of 300 hectares, with the majority consisting of wastewater ponds from this factory (Fijani et al., 2017; Shahbazi et al., 2015). Also, 8000 cubic meters of wastewater flow into these ponds daily (Fijani et al., 2013; Gharebaghi et al., 2009). Most of the water consumed by the factory is obtained from the Alavian dam, underground waters, and fresh drinking water belonging to the city of Maragheh.

On April 25, 2010, five wastewater ponds broke due to spring rains, resulting in a flash flood (Shahbazi et al., 2015). The floodwaters flowed downstream of the factory to the arable lands, causing damage to the vegetation and crops in the area (refer to Figure 2).

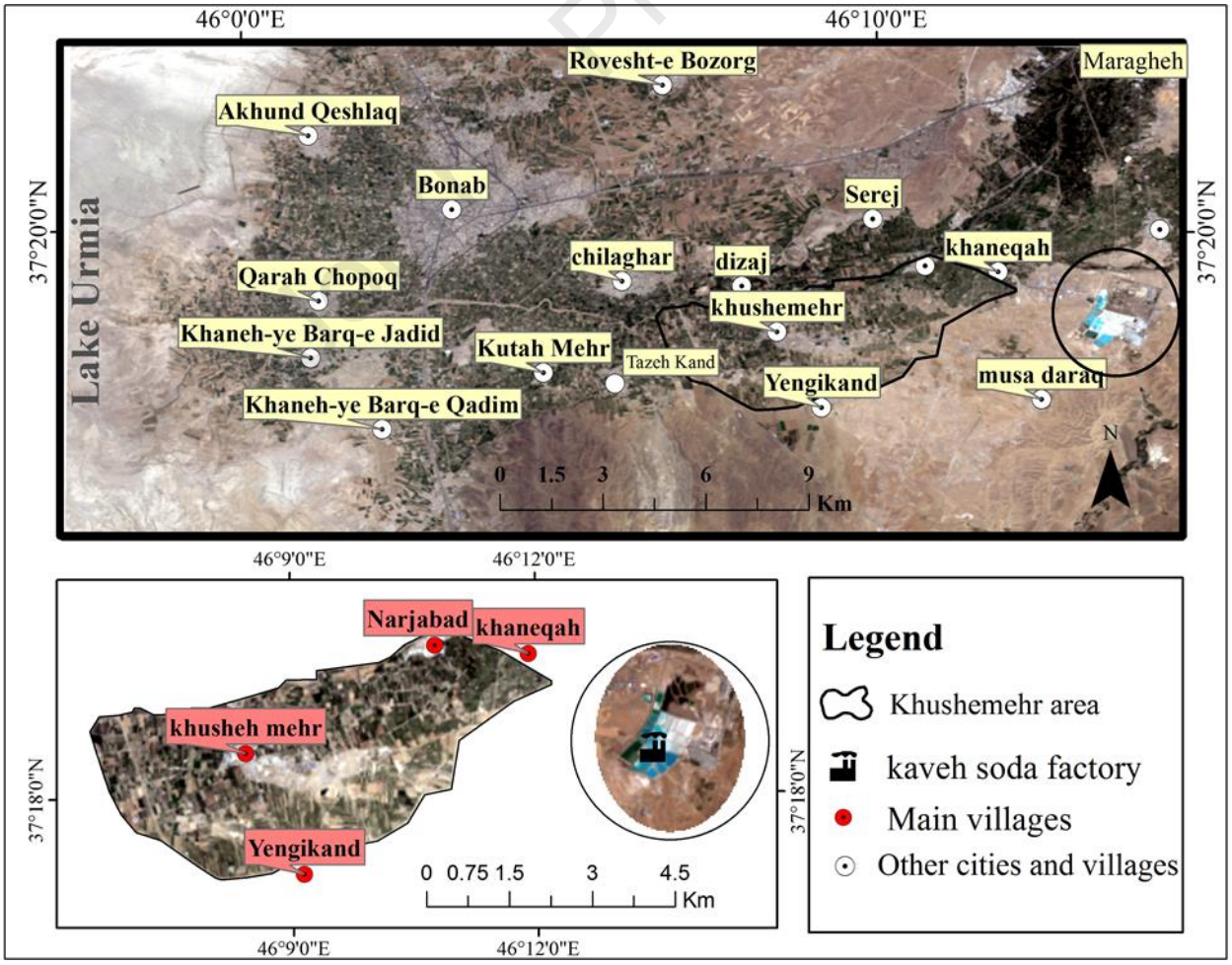

Mehrnooshtahereezadeh@gmail.com

Figure 1. The flooded area (Khusheh Mehr and its surroundings) created from Landsat images.

Figure 2. Image A shows the broken ponds after the flood. Images B, C, and D show the flooded areas of Khusheh Mehr.

3. MATERIALS AND METHODS

3.1. Landsat images

This research utilized image collections (path/row 168/034) obtained from Landsat 5 (TM), Landsat 7 (ETM+), and Landsat 8 (OLI) satellites. However, Landsat 7 images were used less frequently due to the presence of a gap caused by SLC error (Figure 3). These data were processed at Level-2 and downloaded from the USGS Earth Explorer (https://earthexplorer.usgs.gov/). Due to the unavailability of images at regular intervals, the available images were prepared and downloaded for the relevant months. Since the wastewater pond accident occurred in April, the first time series used to assess the vegetation in the area was one month after the flood (May), during which the area showed the maximum size in terms of greenery. The second time series was acquired in July, which had more available images and a lack of cloud cover. The Landsat images from USGS Earth Explorer used for this research are provided in Table 1.

Mehrnooshtahereezadeh@gmail.com

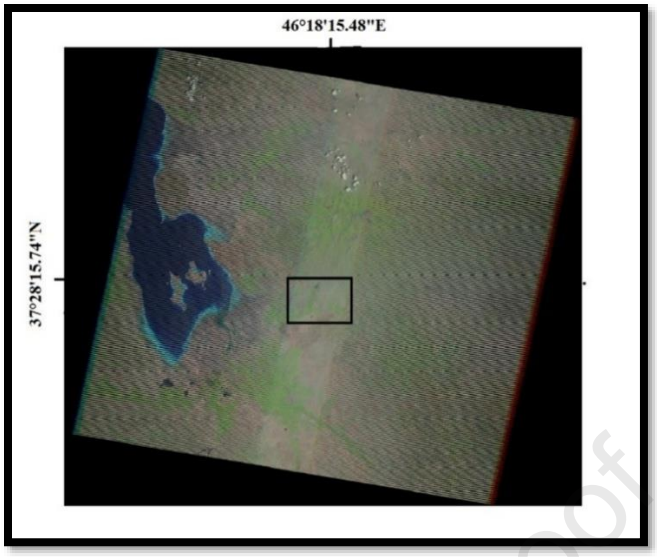

Figure 3. A Landsat 7 image of the central line with no gap on 24/06/2010; Kaveh Soda ponds and Khusheh Mehr area are located here.

3.2. Precipitation data

To demonstrate that rainfall was one of the reasons for the pond breaking and flash flood, daily rainfall data for April 2010 were downloaded for the city of Maragheh from the meteorological data website ("Weather data SYNOPS/BUFR - GFS/ECMWF forecast - Meteomanz.com," n.d.) and are presented in Figure 4-A. In particular, heavy rainfall occurred in the study area in April 2010, especially in the two days before the flood (Figure 4-A), with a total of 23 mm.

This study also examined monthly rainfall data for the month of April in the years before and after the flood to determine the importance of precipitation in the occurrence of the flood (Figure 4-B). The monthly rainfall chart for the entire month of April (April 1 to 31) shows data from 2008-2013, and it is evident that the monthly rainfall of 2010 was significantly higher compared to the same period of the previous two years. It is worth noting that the monthly rainfall for April 2010 was 46.6 mm until the time of the flood on April 25, which is much more than the same period in 2009 with 7.8 mm. Therefore, although rainfall in the two days before the incident was not the only significant factor in the occurrence of this flood, it definitely played a role. The main factor was the increase in the volume of wastewater compared to previous years and the loose soil walls of the ponds (Figure 2-A), with rainfall serving as an aggravating factor.

Mehrnooshtahereezadeh@gmail.com

198

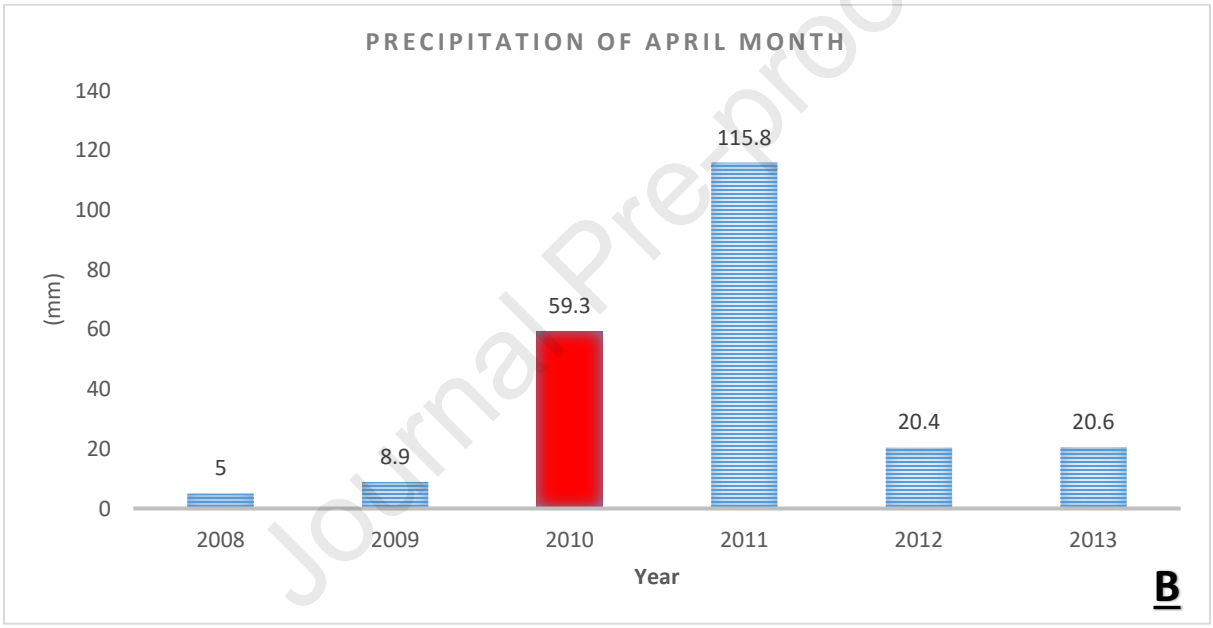

199

200 Figure 4. A: Daily rainfall in April 2010. B: Precipitation totals for April, 2008-2013.

201

202 Table 1. Landsat images used in this study (https://earthexplorer.usgs.gov/).

203

Sites	**Maragheh-Bonab Plain**	**Khusheh Mehr**	
Landsat	5, 8	5, 7, 8	
Date	2001/07/09 2005/07/20 2006/07/23 2009/07/15 2010/07/18 2011/07/05 2013/07/10	2001/07/09 2005/07/20 2006/07/23 2009/07/15 2010/07/18 2011/07/05 2013/07/10	2007/05/23 2009/05/20 2010/05/31 2014/05/26 2019/05/24

Mehrnooshtahereezadeh@gmail.com

	2016/07/18 2019/07/11	2016/07/18 2018/07/08 2019/07/11	

3.3. Topography data

Furthermore, maps and shape files of the channels and main river in the flood area were collected and created to better understand the drainage system over the studied area (Figure 5). In addition, a digital elevation model (DEM) was obtained from the Shuttle Radar Topography Mission (SRTM) 12.5 meters (Lemenkova, 2016; Wu, 2017) to determine the topography and direction of surface water flow (Figure 6).

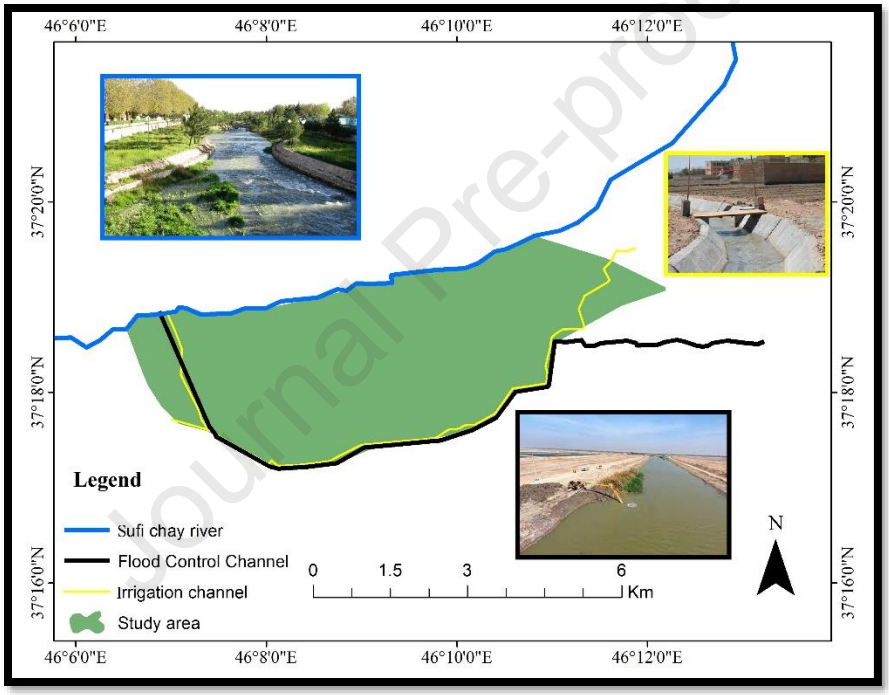

Figure 5. Main rivers and canals of Khusheh Mehr: The Sufi Chay River crosses the Northern area of this region; an irrigation canal shown in yellow color is a canal 1.5 meters in depth and 1 meter width. The drainage channel called flood control, with 4 meters of depth and 10 meters of width begins from the head of Kaveh Soda ponds and runs along the irrigation canal through the South of Khusheh Mehr, reaching the Sufi Chay River.

Mehrnooshtahereezadeh@gmail.com

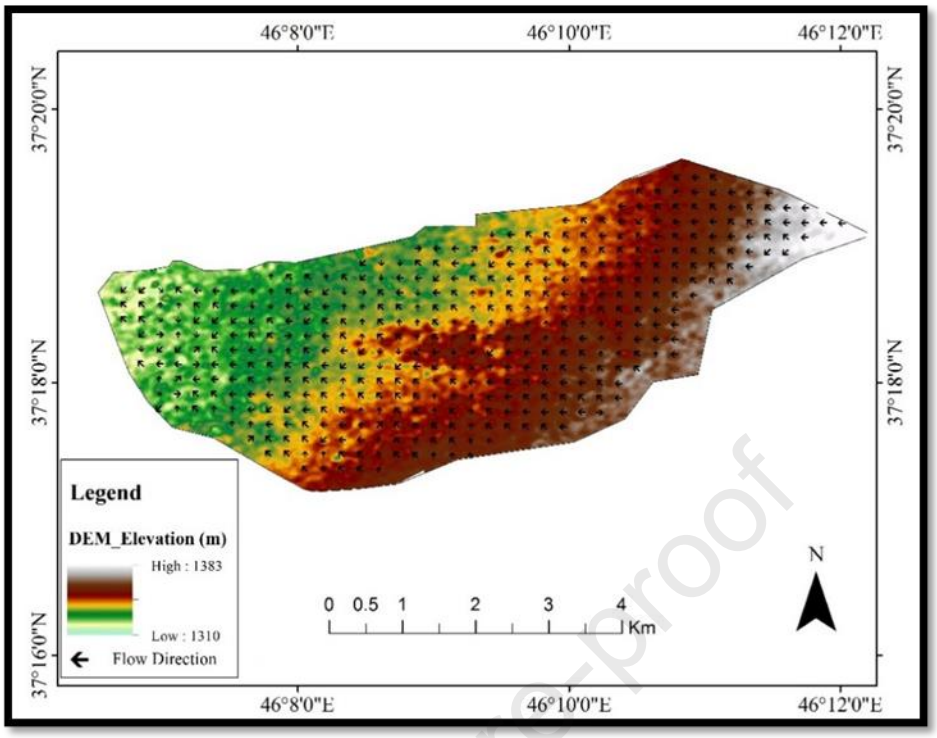

Figure 6. Topography and stream direction: the topography of Khusheh Mehr includes a decrease in altitude from the East in Mount Sahand highs to the West in Lake Urmia. This area's slope and stream direction also are to the West, i.e., Lake Urmia. The maximum altitude of the Khusheh Mehr region is 1383 meters in the East, and its minimum is 1310 meters in the West.

3.4. Methods

Spectral indices, such as NDVI and NDWI, are capable of separating vegetation and water-covered areas from other subjects. In this study, these indices were computed from Landsat images and then classified into certain classes to detect changes in the vegetation and wastewater ponds. The background information on NDVI and NDWI, as well as the classification, sampling, and flood path detection approaches, are briefly described below. Additionally, the flowchart of the actions taken in this study is illustrated in Figure 7.

3.4.1. Normalized difference vegetation index

NDVI is one of the most commonly used indexes for analyzing and dynamically monitoring vegetation on a regional and international scale (Vrieling et al., 2013; Zhu et al., 2013). Introduced by C. J. Tucker in 1979, this index has a numerical value between -1 and +1, with values below zero during the growth season indicating the absence of vegetation (such as deserts, wastelands,

Mehrnooshtahereezadeh@gmail.com

clouds, snow, water, and glaciers), and values above zero and towards +1 indicating vegetation. NDVI was used in this study to show the dispersion and quality of vegetation (Valjarević et al., 2020). The NDVI can be calculated using the following formula (Choubin et al., 2019; Sajedi-Hosseini et al., 2018):

Equation (1) $$NDVI = (NIR-Red)/(NIR+Red)$$

Healthy vegetation exhibits low reflection of light in the red band and higher reflection in the near-infrared band, and hence an increase in the positive value of NDVI indicates growth in green vegetation (Saravanan et al., 2019). The vegetation in the studied area suffered enormous damage after the flood, and therefore, NDVI was used to investigate the impact of the flood on the vegetation in greater detail.

3.4.2. Normalized Difference Water Index

NDWI was introduced by (C. J. Tucker, 1979) to detect surface water and measure its extent. Although this index was designed to work on multi-band Landsat images, it is also effective in analyzing the extent of free water (Murray et al., 2012; Panigrahy et al., 2012). NDWI is calculated using the green and near-infrared bands as:

Equation (2) $$NDWI = (Green-NIR)/(Green+NIR)$$

NDWI values above zero represent water surfaces, while values lower or equal to zero indicate non-water surfaces (McFeeters, 2013). This index was used to analyze changes in wastewater ponds in different years and investigate changes in wastewater before and after the flood in the study area.

3.4.3. Index classification

The purpose of image classification is to sort all image pixels into specific classes or themes. Two commonly used classification approaches are supervised (semi-automated) and unsupervised (automatic) classification (Milanović et al., 2017). In this paper, we used the supervised classification approach. More specifically, the area was classified into strong and dense vegetation (NDVI > 0.3) and weak vegetation (NDVI < 0.3) every year. The average NDVI value was also calculated for different years. Wastewaters were measured for different years and changes in their extent before and after the flood were investigated by classifying NDWI > 0 and NDWI < 0.

Mehrnooshtahereezadeh@gmail.com

3.4.4. The sampling method of vegetation index data (NDVI)

In this study, it was necessary to classify the area's vegetation to measure and compare changes in the extent of vegetation area. Thus, the vegetation had to be separated from urban areas and wastelands before being classified and the vegetation area calculated. As a result, threshold pixels for each year's vegetation from the NDVI images were needed to confirm that the presented pixels were indeed parts of the vegetation.

After calculating NDVI for each year in Maragheh-Bonab Plain, 17500 pixels out of a total of 416816 vegetation pixels were selected as vegetation samples from certain vegetation lands and orchards. To ensure that the selected pixels were definitely vegetation, 10% of the initial pixels of the samples were excluded, and the numerical value of the pixel number 1751 was chosen as the initial vegetation limit in that year. In this manner, the vegetation threshold was obtained by the same method for each year, and then the area of vegetation was classified and calculated.

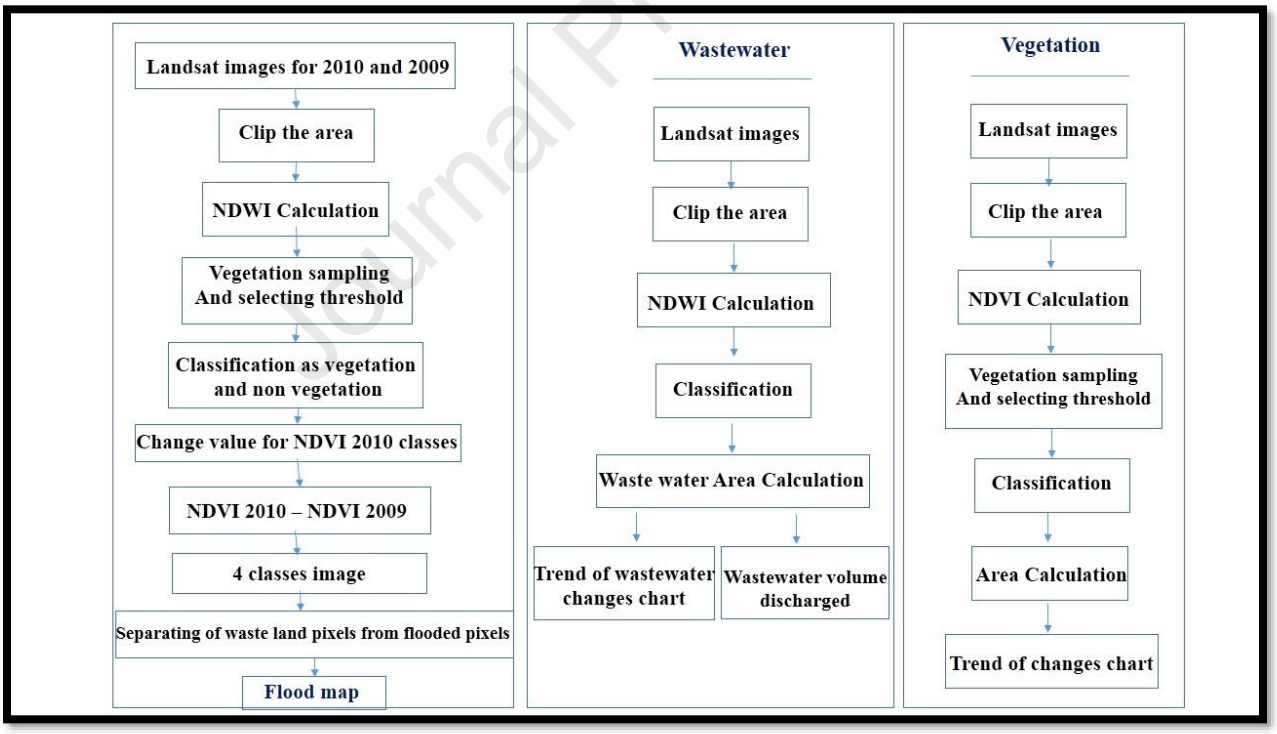

Figure 7. The flowchart of actions taken in this study.

Mehrnooshtahereezadeh@gmail.com

3.4.5. Detection of the flood path

The flood path was detected using NDVI data in May 2009 and May 2010, as this is when the area has the greenest vegetation (maximum spring greenery). This was done by first sampling the vegetation, determining the minimum threshold for vegetation, and then classifying the area into two categories: vegetation and non-vegetation with numerical values of 1 and 2, respectively. For the next step, the NDVI image values for 2010 were classified, and then each value was squared (pixel value * pixel value). Consequently, the numerical values in the classified image for 2009 are 1 and 2, while the values for 2010 are 1 and 4 (refer to Table 2). Finally, a four-class image was gained by subtracting pixels (classified NDVI 2010 – classified NDVI 2009) (refer to Table 3).

Table 2. Numerical values in classified images.

	Non-vegetated land pixel numerical value	Vegetation pixel numerical value
Classified NDVI of 2009	1	2
Classified NDVI of 2010	1	2
2010 classified NDVI after pixel value changes	1	4

Table 3. The resulting classes after subtraction of the images (pixel calculations).

2010	**Manipulation**	**2009**	**Result**	**Result image function**
Vegetated (4)	-	Vegetated (2)	2	Vegetated (No flooded)
Vegetated (4)	-	Non-vegetated (1)	3	Vegetated (No flooded)
Non-vegetated (1)	-	Vegetated (2)	-1	Flooded
Non-vegetated (1)	-	Non-vegetated (1)	0	(Wasteland /residential) or flooded

From Table 3, despite the three-class functions are precisely determined, the exact nature of one class remained unknown (i.e., pixel with zero numerical value). Therefore, further steps were implemented to detect the flooded areas. In the resulting image after the operation mentioned above, pixels with zero numerical values were chosen, separated and considered as an independent layer. For the next step, based on the knowledge of the region and how far the flood has progressed

Mehrnooshtahereezadeh@gmail.com

from the flood control channel in different areas of the Khusheh Mehr, three buffers with a radius of 1200, 1000, and 400 meters were applied over the flood control channel mentioned in Figure 5. Therefore, zero-layer pixels within this region were considered flood pixels while those outside the buffer line were classified as wasteland or residential.

4. RESULTS AND DISCUSSION

4.1. Wastewater

4.1.1. The trend of changes in wastewater areas

The area of wastewater in the ponds was calculated using NDWI derived from Landsat images. The results showed that the volume and size of industrial wastewater from the factory have had an upward trend over the past years (Figures 8 and 9). Specifically, the area of industrial wastewater has increased from 43.47 hectares in 2005 to 115.56 hectares in 2021, and assuming an average depth of 8 meters for all ponds, a total of 9244800 cubic meters of industrial wastewater has accumulated in these ponds over time. Furthermore, the temporal trend of changes in the industrial wastewater area was analyzed using a linear regression model, as illustrated in Figure 8. The results indicate a significant increasing trend, as demonstrated by the regression coefficient (slope ≈ 9.34), which is significantly different from zero at the 95% confidence level (p-value ≈ 0.001).

Mehrnooshtahereezadeh@gmail.com

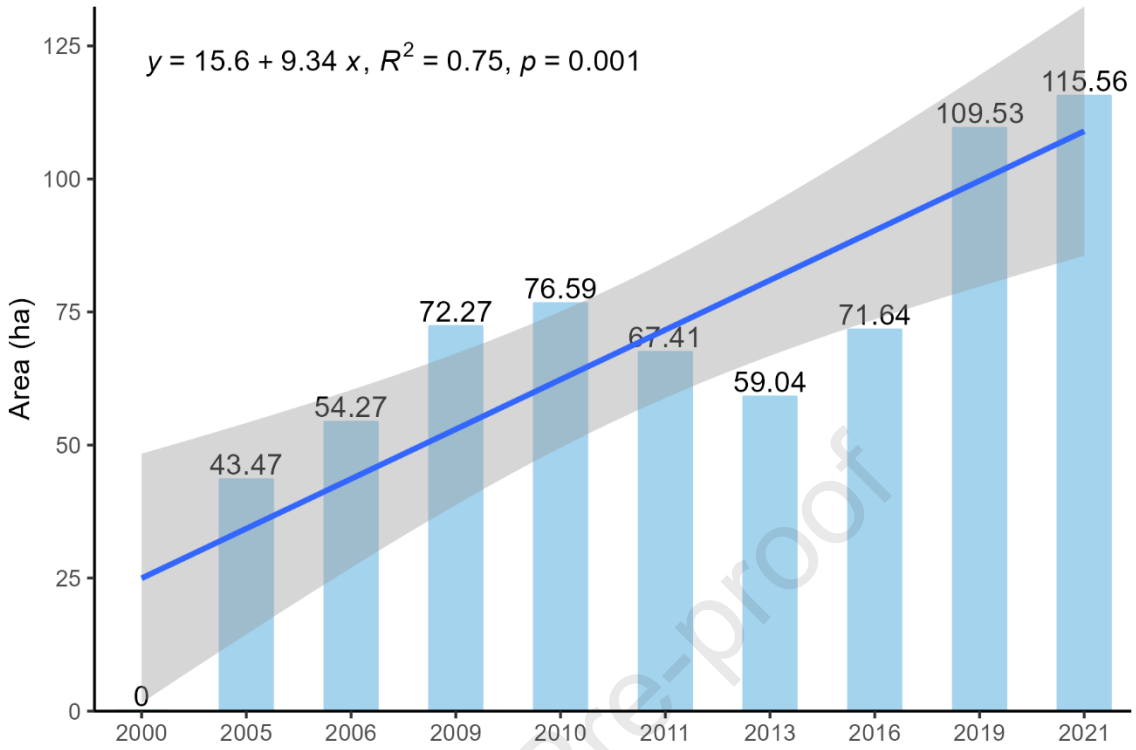

Figure 8. The trend for the area of industrial wastewater changes in Kaveh Soda factory ponds during the period 2000 to 2021.

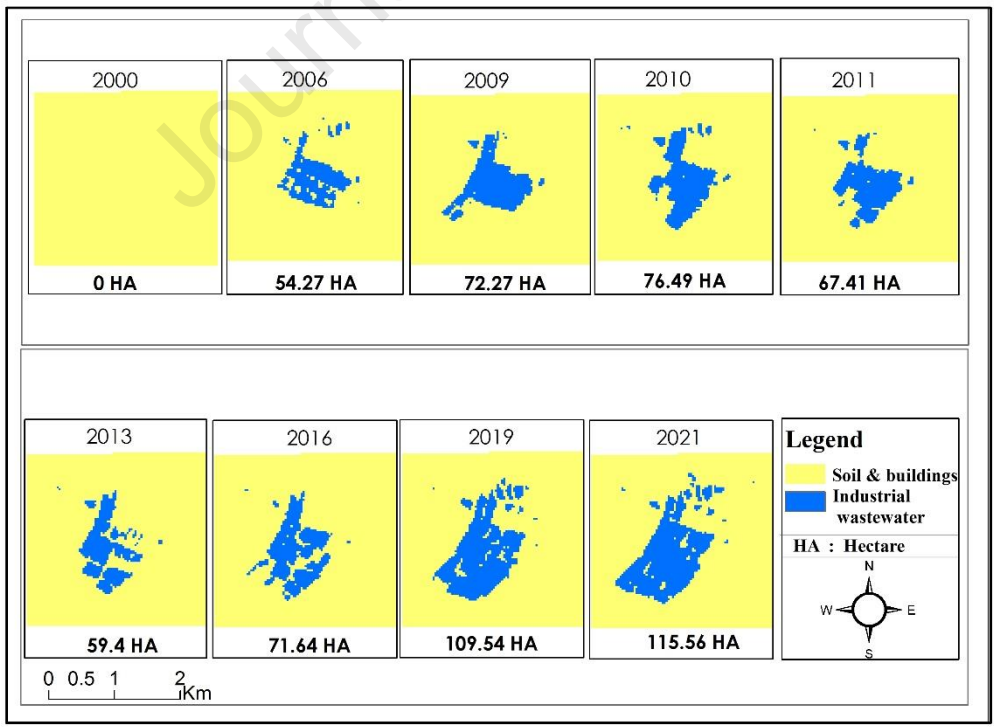

Mehrnooshtahereezadeh@gmail.com

Figure 9. The trend of changes in industrial wastewater in Kaveh Soda Factory from 2000 to 2021 using NDWI derived from Landsat images.

The increasing extent of Kaveh Soda's industrial effluent poses a serious threat to the environment in the region. In the event of a flood similar to the one that occurred in 2010, there is a possibility of severe damage to the area, both financial and human. This is why the increasing volume and extent of wastewater year by year leading to the potential for more severe and larger floods is of concern.

4.1.2. Changes in the volume and area of wastewater before and after the event

Analysis of images from before and after the flood in 2010 using NDWI shows a decrease in the area of factory wastewater in the south-western parts of the ponds (Figure 10). After the flood, the area of industrial wastewater decreased to 15.66 hectares. Considering an average depth of 8 meters of ponds in the mentioned area, nearly 1250000 cubic meters of wastewater has been discharged into the studied area, in the period from April to June 2010. The runoff from the flood has flowed into the rural areas of Khaneqah, Narjabad, YengiKand, and Khusheh Mehr due to the topographic slope (Figure 6). The channel for controlling the flood and the Sufi Chay River (Figure 5) have forwarded the main body of the wastewater to Lake Urmia. However, the flood-damaged agricultural lands are heavily affected, causing serious problems for the vegetation in the Khusheh Mehr, Khaneqah, Narjabad, and YengiKand rural areas.

Mehrnooshtahereezadeh@gmail.com

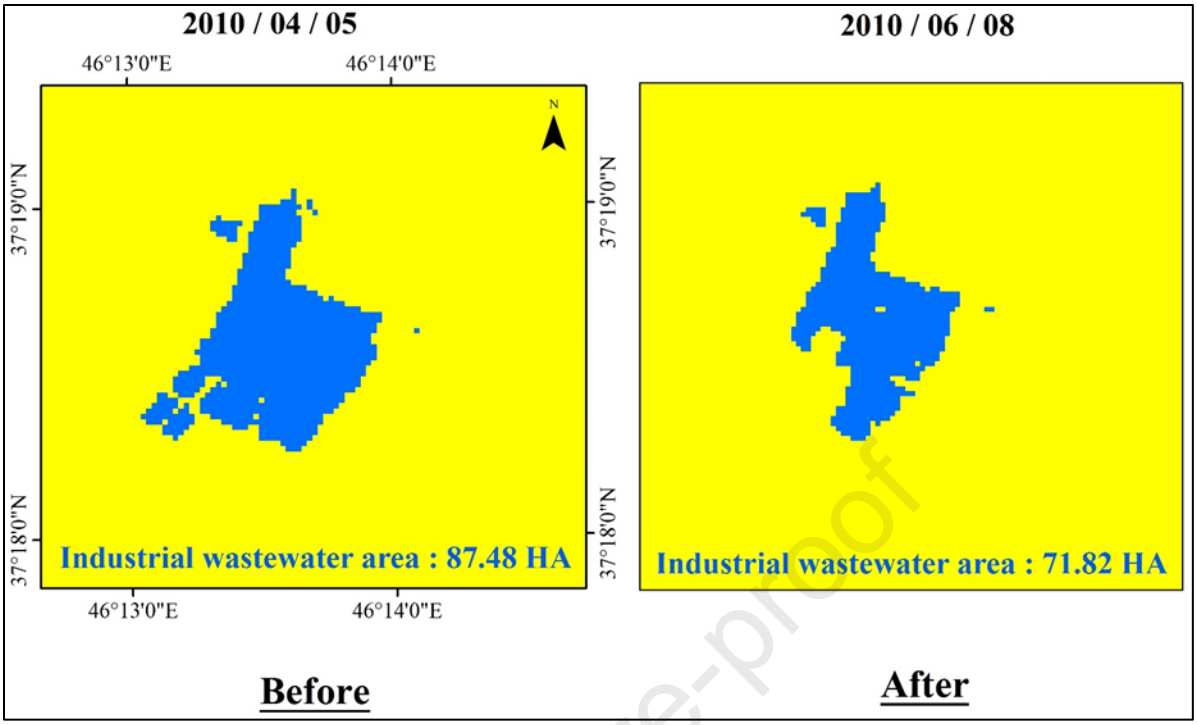

Figure 10. The area of the industrial wastewater before and after the flood in 2010 using NDWI derived from Landsat images.

4.2. Flood path

Figure 11 shows the land use map of Khusheh Mehr before the 2010 flood. The results of flood detection revealed that 538 hectares of agricultural lands in this region were directly affected by the floods (Figure 12). It is worth considering that the flood control channel and the Sufi Chay River played a crucial role in controlling and directing the flood. Due to the region's topography (Figure 6), the flood entered the Sufi Chay River from the northeast of Khusheh Mehr after crossing through Khaneqah, Narjabad, Khusheh Mehr, and YangiKand rural areas. In the south-eastern and southern parts of Khusheh Mehr, the flood control channel and irrigation channel are located (Figure 5). The flood control channel directed a significant part of the flood toward the Sufi Chay river and, consequently, Lake Urmia located in the western side of the study area.

Apart from contaminating the soil and destroying vegetation, the flood contaminated the groundwater aquifer as well. The underground water in the region lost its quality and potability due to the intrusion of the flood in some parts of the studied area. Previously, farmers and landowners used well water for drinking and consumption, which they had dug for agricultural purposes. According to the statements of local farmers, the use of well water in some areas of the

Mehrnooshtahereezadeh@gmail.com

region to irrigate vegetation caused the remaining trees and gardens to dry up. This flood not only had apparent impacts on the vegetation of Khusheh Mehr and caused severe damage to the ecosystem, but also had long-term effects on the underground water, which needs to be investigated in future studies**.** Hence, laboratory research should be conducted. In previous years, two studies were conducted on the infiltration of the factory's wastewater into the underground waters of Khusheh Mehr through ponds and as a result of this flood (Fijani et al., 2013, 2017).

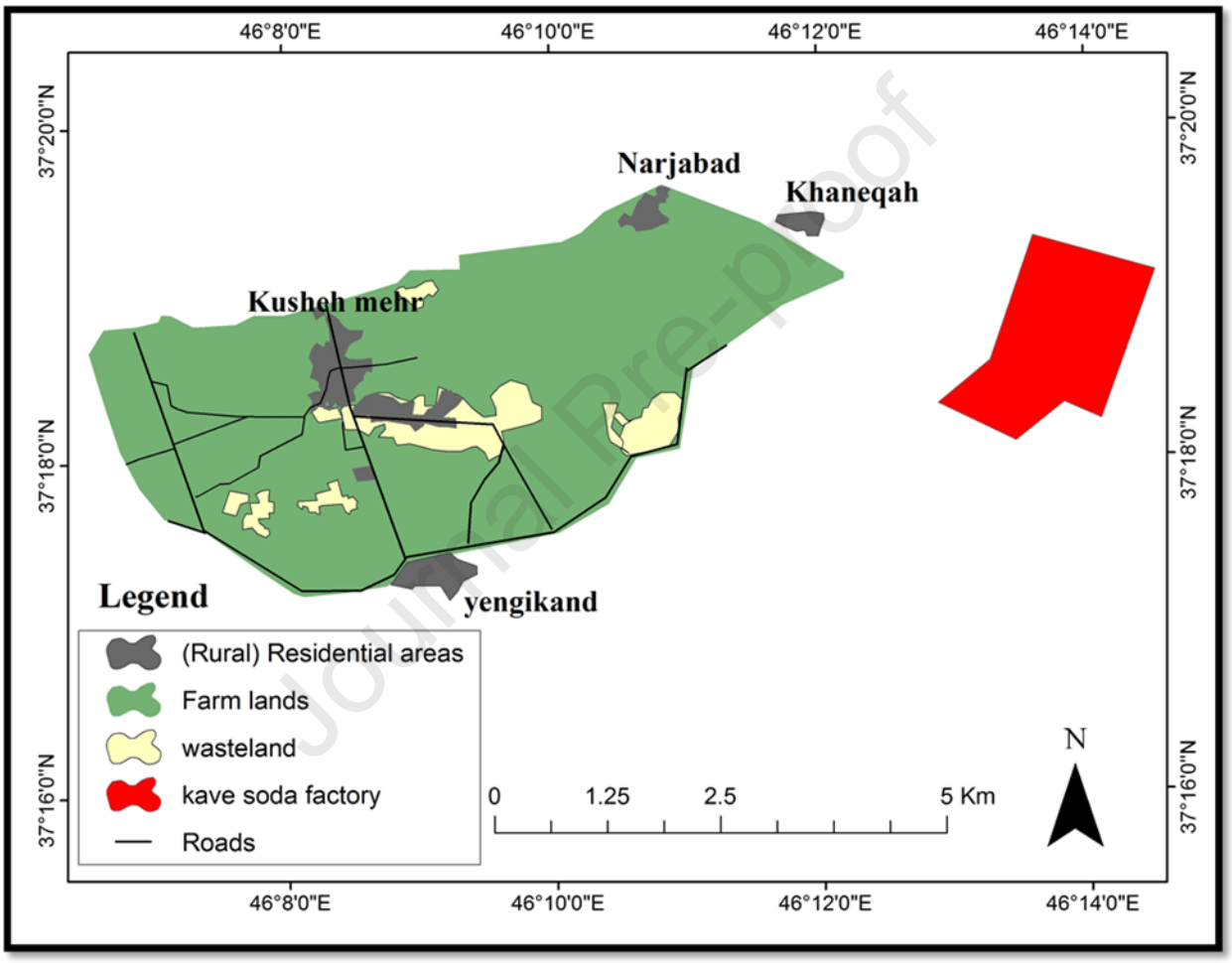

Figure 11. Land use and land cover in the study area before the flood in 2010.

Mehrnooshtahereezadeh@gmail.com

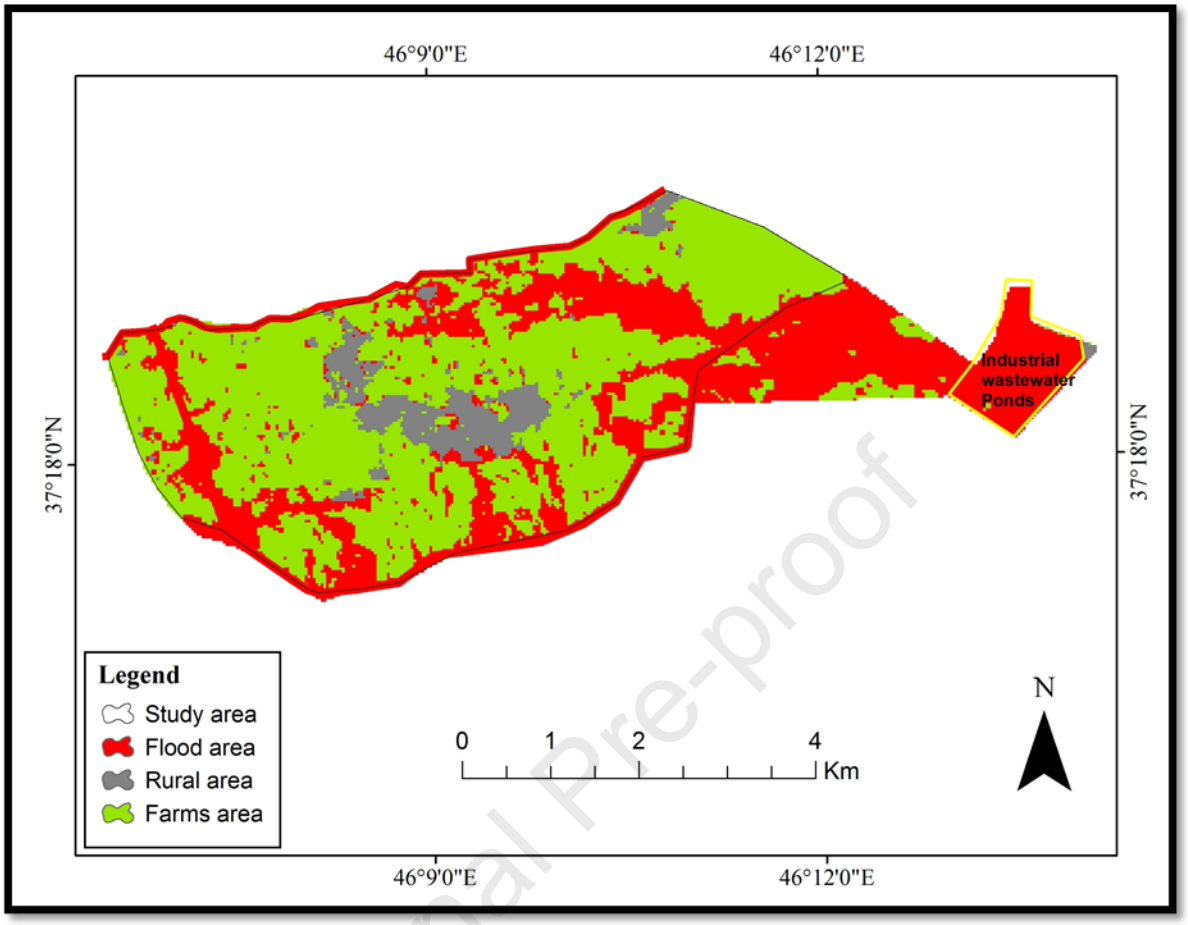

Figure 12. Flood path crossing lands of Khusheh Mehr (Khusheh Mehr, YengiKand, Narjabad and Khaneqah) derived from Landsat images.

Previously published research has demonstrated that the underground water in the Khusheh Mehr region and its surrounding areas has been contaminated by industrial wastewater from the Kaveh Soda factory, resulting in a significant increase in chloride ions (Cl), calcium (Ca), sodium (Na), and sulphate (SO4) levels after the establishment of the factory and the 2010 flood. The rise in these ions has led to an increase in the electrical conductivity (EC) of the groundwater. According to sampling data, 20% of the groundwater has poor quality due to factory wastewater (Fijani et al., 2017).

4.3. The vegetation

4.3.1. The trend of vegetation changes in the area of Khusheh Mehr and surrounding rural areas (The flood's epicentre).

Mehrnooshtahereezadeh@gmail.com

372 To analyze the impact of the flood on the vegetation of the Khusheh Mehr region and surrounding
373 rural areas, Landsat images captured in May and July were used. The results of the NDVI analysis
374 in May of subsequent years revealed a decline in both the quality and quantity of vegetation in
375 Khusheh Mehr and the rural areas affected by the flood. The area covered with dense vegetation
376 (NDVI > 0.3) decreased to 21.8 hectares in May 2010, which was a significant reduction compared
377 to the 245 hectares in 2009 (Figure 13 and Figure 14), corresponding to a decline of 91%.
378 Moreover, the total vegetation area calculated for each year showed that the vegetation area for
379 the flood year had decreased by 249 hectares compared to 2009, a 15% decrease.
380

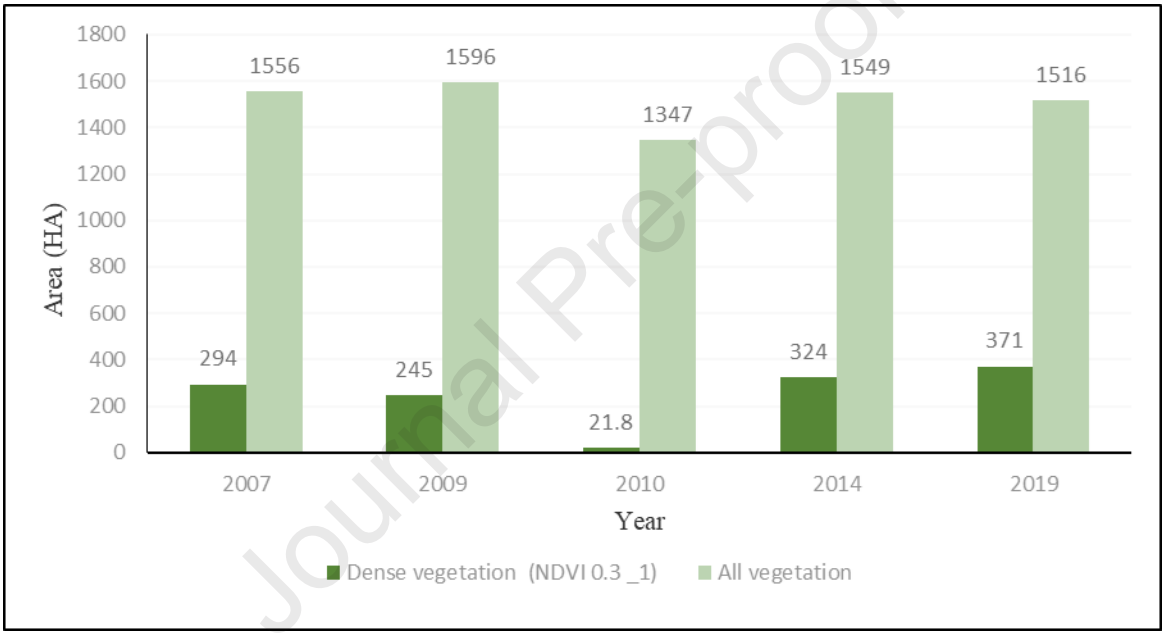

381
382 Figure 13. The trend for changes in the dense vegetation and overall vegetation in the Khusheh
383 Mehr region in years before and after the flood in 2010 using NDVI index in May.

Mehrnooshtahereezadeh@gmail.com

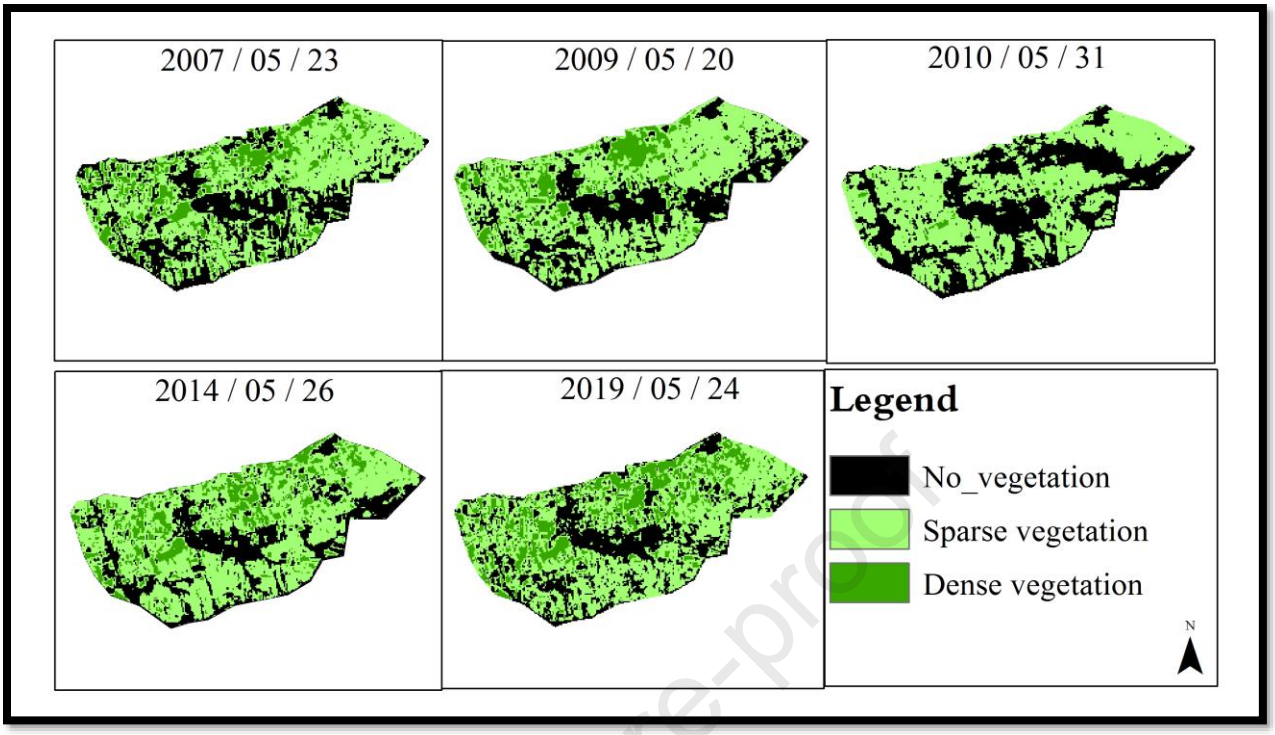

Figure 14. The vegetation map of the Khusheh Mehr region in May of different years derived from Landsat images.

The vegetation changes for July were also analyzed over the last 20 years (Figure 15 and Figure 16). In the years 2010 and 2011, the area of dense vegetation surfaces (NDVI > 0.3) experienced a significant drop compared to 2009 and 2006, corresponding to a 55% decrease. In addition, the entire vegetation area of Khusheh Mehr and its surrounding rural areas experienced a 29% and 17% decline in July compared to 2006 and 2009, respectively. Due to this flood, the vegetation in areas affected by industrial flood was completely destroyed, and the soil where the flood had crossed lacked desirable vegetation for one to two years. However, the vegetation and greenery of the area were restored before the flood through deep plowing, adding 10-20 centimeters of fresh soil, adding animal fertilizer to fields, continuous irrigation, and natural recovery of the land itself over time. But according to local reports from farmers, the quantity and quality of agricultural products decreased after the floods.

Mehrnooshtahereezadeh@gmail.com

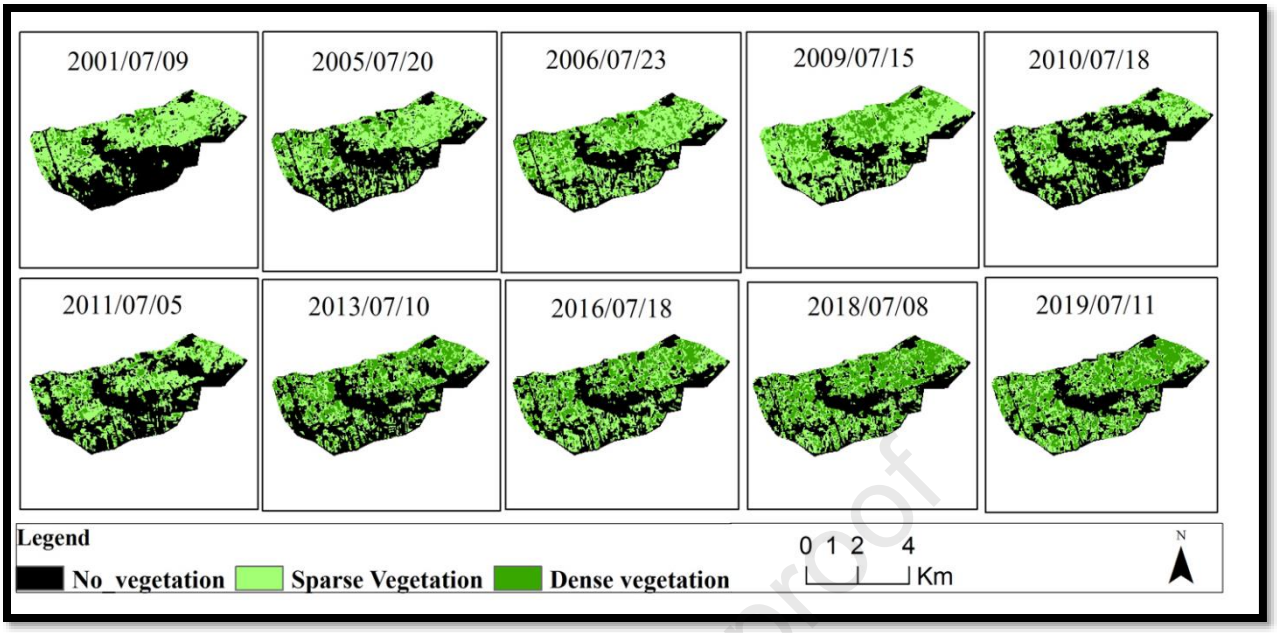

Figure 15. The vegetation map of the Khusheh Mehr region in July of different years. Derived from Landsat images.

The maps (Figure 15) for the years 2010 and 2011 showed that the non-vegetation areas surrounding Khusheh Mehr have expanded as a result of the industrial wastewater flood from the Kaveh Soda factory. Additionally, according to the results (Figure 16), the whole vegetation and dense vegetation areas in 2010 and 2011 have shown a noticeable decline. The lowest area of whole vegetation covered in the studied years related to the years 2010 and 2011 was 955 and 960 hectares, respectively, which is the lowest amount among the studied years. In addition, the dense vegetation area in the two years mentioned above showed a significant decrease compared to previous years, reaching 182 and 179 hectares.

In 2001, there were extensive non-vegetated lands in the south of Khusheh Mehr due to the lack of agricultural prosperity and irrigation channels during those years. It should be noted that the east, west, and north of Khusheh Mehr have higher-quality soil compared to the south. Later, with an increase in the use of underground waters and canalization of the dam water to irrigate the southern areas of Khusheh Mehr, the southern parts of Khusheh Mehr became grape gardens, apple orchards, and other vegetable fields with rich vegetation.

Mehrnooshtahereezadeh@gmail.com

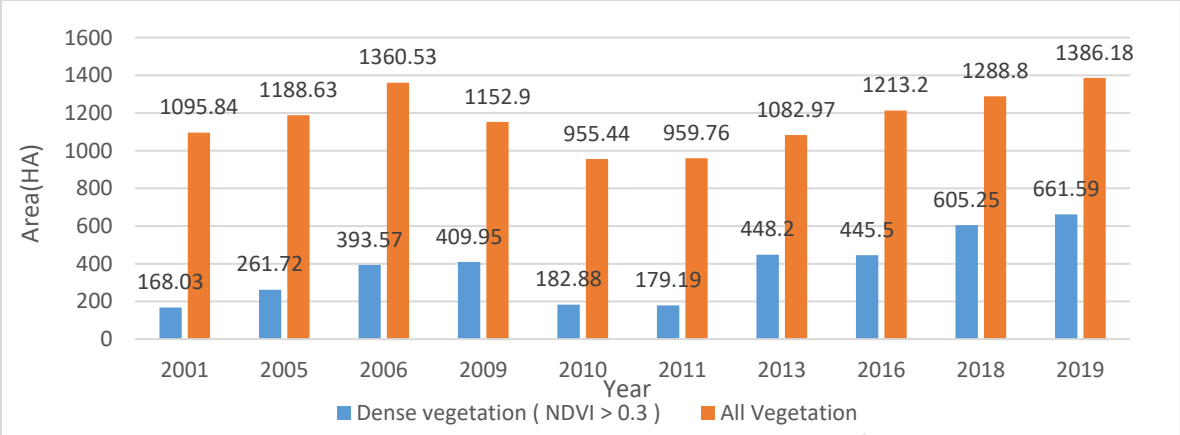

Figure 16. The trend for changes in the dense vegetation and the whole vegetation in general surrounding Khusheh Mehr in the years before and after the flood in 2010 using NDVI in July.

4.3.2. Trends for changes in the vegetation of the Maragheh-Bonab Plain

The July vegetation was also analyzed to investigate the effects of the flood on the Maragheh-Bonab Plain. The results showed that the general and dense vegetation in 2010 and 2011 had significantly decreased compared to previous years. Specifically, the area of dense and strong vegetation in 2010 decreased by 26% and 21% compared to 2009 and 2006, respectively (Figure 17). However, there was no significant change observed in the overall surface of vegetation. The NDVI image of the Maragheh-Bonab Plain after the 2010 flood is shown in Figure 18, where the ponds and flood path are visibly apparent on the right side of the image.

Mehrnooshtahereezadeh@gmail.com

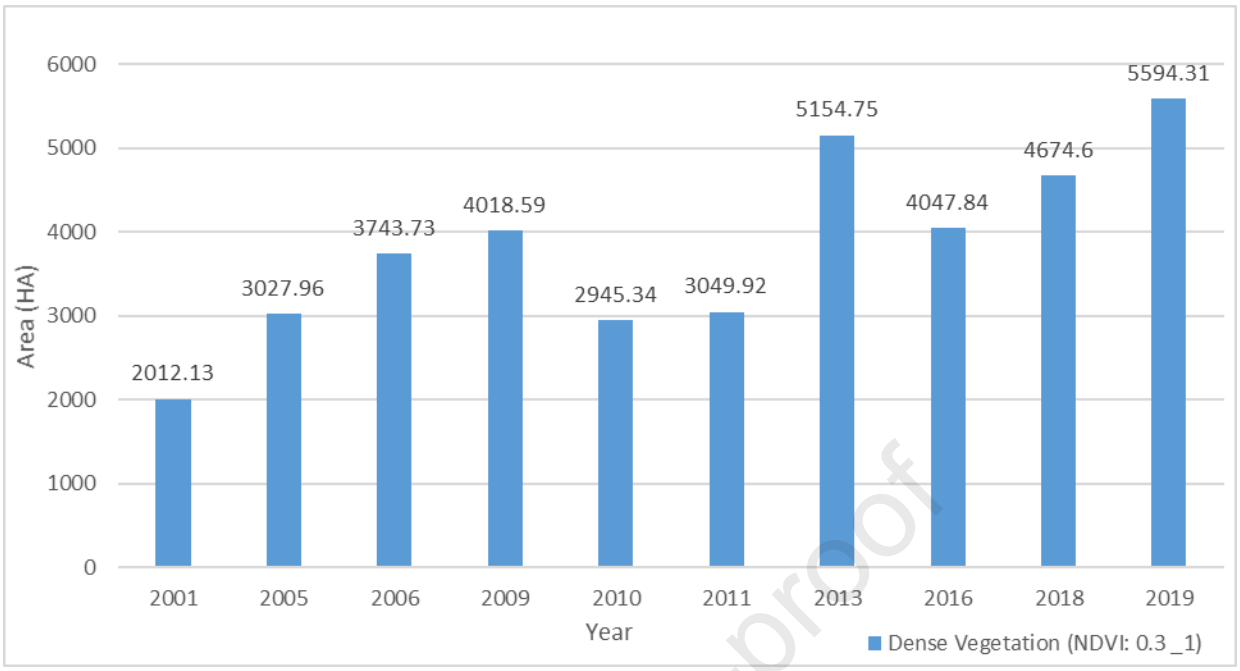

Figure 17. The trend for the changes in the area of dense vegetation in the Maragheh-Bonab Plain region during the years before and after the flood in 2010 using July NDVI.

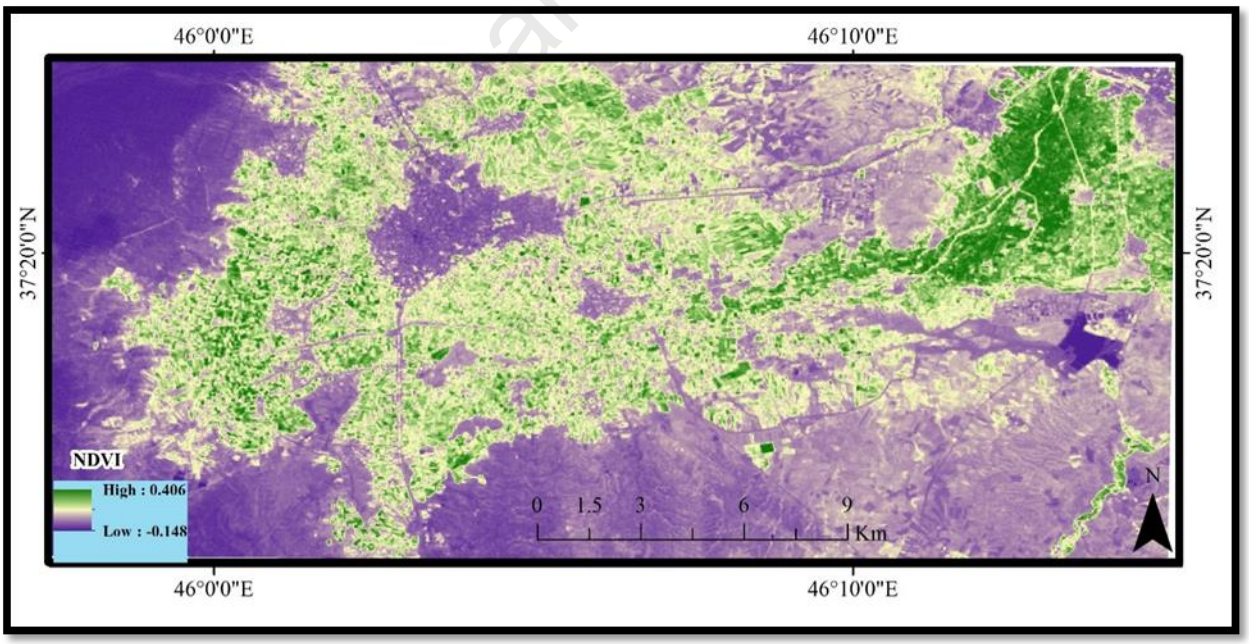

Figure 18. The image resulted from NDVI of Maragheh-Bonab Plain in the flood year (2010) derived from Landsat image.

In the following, the trend of changes in the vegetation area of the Khusheh Mehr region with the trend of vegetation changes in the Maragheh-Bonab plain by the linear regression model was

Mehrnooshtahereezadeh@gmail.com

435 statistically analyzed, and according to the result, the p-value≤0.001 shows a significant trend. In
436 addition, the regression value of 0.91 between the aforementioned data shows a high correlation
437 between the two groups of data.

438 *4.3.3. Vegetation index average*

439 The results of the mean NDVI from the Khusheh Mehr region in May show a decrease in this value
440 in 2010 due to floods. Therefore, the average vegetation index in May 2010 has the lowest value
441 among the studied years (Table 4). A comparative analysis was conducted by calculating the
442 averages of pixels chosen as vegetation pixels in July. The results indicate a rising trend in the
443 average vegetation index (NDVI), but in the years 2010 and 2011, this trend experienced a decline,
444 due to the increase in non-vegetated pixels in the region (Figure 19).

445 Table 4. Table of average vegetation index (NDVI) in Khusheh Mehr area for May of different
446 years.

Year	Mean of NDVI
2007	0.197
2009	0.169
2010	0.165
2014	0.196
2019	0.216

447

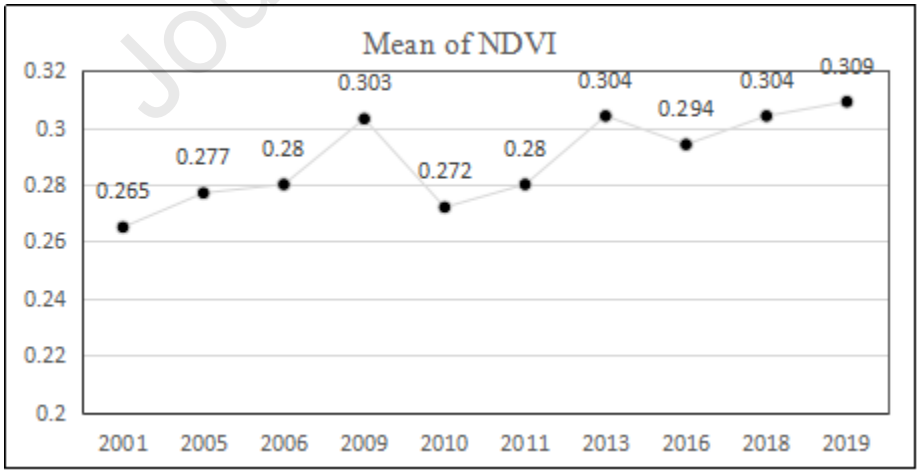

448

449 Figure 19. The chart for the trend showing changes in vegetation index (Mean of NDVI) related
450 to sample pixels of July.

451

452 **5. Recommendations and Limitations**

Mehrnooshtahereezadeh@gmail.com

5.1. Recommendation

Industrial flash floods can have significant negative effects not only on vegetation, which has been analyzed in this study, but also on groundwater and soil quality, leading to long-term environmental and economic problems. This article examines the consequences of the breaking of only five ponds of industrial wastewater from a factory. It highlights that in case of an accident such as an earthquake or torrential rains, the breaking of the ponds is inevitable given the volume of stored wastewater of the factory. A study that estimates the extent to which financial and human losses will increase and how much soil will be contaminated if 20 ponds break is required.

Flash floods can carry pollutants such as chemicals, heavy metals, and other harmful substances that can contaminate groundwater and soil, persisting in the environment for extended periods and posing health risks to humans and animals (Basahi et al., 2018; Masoud et al., 2018). Furthermore, the force of the floodwater can erode soil and wash away topsoil, which can impact the soil's ability to retain moisture and nutrients (Akuja et al., 2001; Getnet et al., 2022; Kathwas et al., 2022). Additionally, flash floods can alter soil structure and cause compaction, reducing the soil's capacity to retain air and water, thereby decreasing its fertility (Kourgialas et al., 2012). This method is especially helpful for analyzing industrial flash floods, which frequently have a significant regional impact. The health and density of the vegetation in the impacted area can be evaluated using NDVI. By this index, the severity of flood damage and the possibility of soil pollution can be found in changes in the health of the vegetation.

The flood happened in 2010, but this research was conducted in 2022-2023. Therefore, when conducting this research, the area had changed entirely compared to the flood period and when it was damaged. The land and vegetation of the area were similar to the state before the flood, and the land had considerably recovered. Using the archived Landsat images, we were able to examine the continuous changes in the vegetation cover of the Khusheh Mehr. In this regard, valuable maps and data were obtained. Also, due to the special conditions of the factory and the sensitivity of the officials, it is not possible to physically enter and leave the site, but with using satellite images, we extracted the extent and volume of sewage in different years using remote sensing indicators. The things mentioned in this research provided us with a more comprehensive and accurate view of the extent of changes in vegetation and effluents, which would not have been possible without remote sensing.

Mehrnooshtahereezadeh@gmail.com

Finally, the results of the current study will assist scientists and managers of flood hazards in assessing the vulnerability of floods and in making decisions about how to manage and lessen the effects of flood events. It recommends that the proposed method, a reliable instrument that can effectively assess the impact of industrial floods on vegetation in different areas. Remote sensing is an economical technique for analyzing industrial flash floods. It does away with the necessity for time- and money-consuming ground-based surveys.

5.2. Limitations

The study has encountered several restrictions including a lack of access to complete information. In fact, researchers were not allowed to enter the factory for field visits in order to access information such as the exact volume of wastewater as well as water consumption, which is derived from Sahand springs and underground waters. It would have been helpful to obtain a report from the factory detailing the precise amount of wastewater produced to make more accurate calculations.

In terms of remote sensing, it was not possible to extract the type of solutes and compounds of this factory's effluent, because we used Landsat images with a resolution of 30 * 30 meters in this work, and this was practically not possible whit Landsat images. It was not possible to assess the exact amount of damage to the texture and quality of the soil in terms of remote sensing measurement, and this required laboratory work after the flood. Further, the NDVI is calculated according to the difference between near-infrared and visible red light reflectance, which is significantly impacted by vegetation. As a result, it is less efficient in identifying flood damage in regions with scant or no vegetation. Also, NDWI can identify water bodies, although the water's depth or speed may not be precisely measured because of the limitation.

6. CONCLUSION

The Kaveh Soda factory in Maragheh was established in 2004 to produce light and heavy sodium carbonate, as well as soda. However, the factory's industrial wastewaters have become one of the biggest environmental challenges for water resources and soil in the Maragheh–Bonab plain, particularly in rural areas like Khusheh Mehr. The factory produces 8000 liters of wastewater with high EC (over 200 micro siemens) per day. In April 2010, several wastewater ponds broke, causing a flash flood of dangerous wastewater to flow into the surrounding rural areas and agricultural lands.

Mehrnooshtahereezadeh@gmail.com

This study examined the impact of the flash flood on the region's vegetation structure at both the local and regional levels using Landsat 5, 7, and 8 satellite images from 2000-2020. The results showed that on a local level (agricultural lands and orchards in the region of Khusheh Mehr), the average arable land area with dense vegetation index (NDVI > 0.3) was between 250 and 300 hectares. However, in May 2010, dense vegetation in the Khusheh Mehr area decreased by 90% to 21 hectares due to the flash flood. This effect was retrievable in July 2010 and 2011 when the vegetation of rural areas of Khusheh Mehr experienced a fall of at least 50% compared to the same months in 2006 and 2009. This significant decrease in dense vegetation surface on a local scale is due to the direct impact of contaminated factory runoff and increased soil EC.

The study findings were consistent on a regional scale (Maragheh – Bonab plain). Statistical analysis with a regression of 0.91 confirmed the high correlation between them. Dense vegetation (mostly agricultural lands and orchards with NDVI > 0.3) underwent a decrease of at least 1,000 hectares in July 2010 and 2011 and fell to less than 3,000 hectares in these years compared to an average of 3,900 hectares in 2006-2009. On this scale, the contamination of underground and surface waters due to an increase in water resource EC with factory wastewater after the April 2010 flood clearly affected the vegetation. Soil damage in 2010 caused the entire vegetation and trees that were in direct contact with the flood to dry up. However, in the following years, with some activities of farmers, the vegetation, cultivation, and agriculture gradually returned to their pre-flood status. The financial loss, estimated at 23 million USD after field visits to flooded lands in 2010, was paid to farmers according to experts.

Ethical statement for Remote sensing applications: Society and Environmental

Hereby, I /Mehrnoosh Taherizadeh/ consciously assure that for the manuscript/ Revealing the effect of an industrial flash flood on vegetation area: A case study of Khusheh Mehr in Maragheh-Bonab Plain, Iran/ the following is fulfilled:

1)This material is the author’s own original work, which has not been previously published elsewhere.

2)The paper is not currently being considered for publication elsewhere.

3)The paper reflects the author’s own research and analysis in a truthful and complete manner.

Mehrnooshtahereezadeh@gmail.com

Authors statement

Mehrnoosh Taherizadeh: Conceptualization, Methodology, writing-original draft preparation, Software.

Javid Hojabri Khushemehr: Conceptualization, Contributed to the writing, Data Acquisition, Methodology, Visualization, Software.

Arman Niknam: Analysis, Discussion, Resources, Writing Editing and Reviewing.

Thong Nguyen-Huy: Analysis, Writing- Reviewing and Editing, Supervision.

Gabor Mezosi: Writing- Reviewing and Editing, Supervision.

Declaration of competing interest

The authors declare that they have no known competing financial interests or personal relationships that could have appeared to influence the work reported in this paper.

REFERENCES

Ahmed, K.R., Akter, S., 2017. Analysis of landcover change in southwest Bengal delta due to floods by NDVI, NDWI and K-means cluster with landsat multi-spectral surface reflectance satellite data. Remote Sens. Appl. Soc. Environ. 8, 168–181. https://doi.org/10.1016/j.rsase.2017.08.010

Akuja, T., Avni, Y., Zaady, E., Gutterman, Y., 2001. Soil Erosion Effects as Indicators of Desertification Processes in the Northern Negev Desert 595-. https://doi.org/10.13031/2013.4847

Ali, S.M., Pervaiz, A., Afzal, B., Hamid, N., Yasmin, A., 2014. Open dumping of municipal solid waste and its hazardous impacts on soil and vegetation diversity at waste dumping sites of Islamabad city. J. King Saud Univ. - Sci. 26, 59–65. https://doi.org/10.1016/j.jksus.2013.08.003

Anusha, N., Bharathi, B., 2020. Flood detection and flood mapping using multi-temporal synthetic aperture radar and optical data. Egypt. J. Remote Sens. Sp. Sci. 23, 207–219. https://doi.org/10.1016/j.ejrs.2019.01.001

Arvind, C.S., Vanjare, A., Omkar, S.N., Senthilnath, J., Mani, V., Diwakar, P.G., 2016. Flood Assessment using Multi-temporal Modis Satellite Images. Procedia Comput. Sci. 89, 575–586. https://doi.org/10.1016/j.procs.2016.06.017

Asghari Moghaddam, A., Fijani, E., Nadiri, A., 2015. Optimization of DRASTIC Model by Artificial Intelligence for Groundwater Vulnerability Assessment in Maragheh-Bonab Plain. Sci. Q. J. Geosci. 24, 169–176. https://doi.org/10.22071/GSJ.2015.43279

Ashok, A., Rani, H.P., Jayakumar, K. V., 2021. Monitoring of dynamic wetland changes using NDVI and NDWI based landsat imagery. Remote Sens. Appl. Soc. Environ. 23, 100547. https://doi.org/10.1016/j.rsase.2021.100547

Avand, M., Kuriqi, A., Khazaei, M., Ghorbanzadeh, O., 2022. DEM resolution effects on machine learning performance for flood probability mapping. J. Hydro-Environment Res. 40, 1–16. https://doi.org/10.1016/j.jher.2021.10.002

Mehrnooshtahereezadeh@gmail.com

Azam, M., Kim, H.S., Maeng, S.J., 2017. Development of flood alert application in Mushim stream watershed Korea. Int. J. Disaster Risk Reduct. 21, 11–26. https://doi.org/10.1016/j.ijdrr.2016.11.008

Barzegar, R., Fijani, E., Asghari Moghaddam, A., Tziritis, E., 2017. Forecasting of groundwater level fluctuations using ensemble hybrid multi-wavelet neural network-based models. Sci. Total Environ. 599–600, 20–31. https://doi.org/10.1016/j.scitotenv.2017.04.189

Basahi, J.M., Masoud, M.H.Z., Rajmohan, N., 2018. Effect of flash flood on trace metal pollution in the groundwater - Wadi Baysh Basin, western Saudi Arabia. J. African Earth Sci. 147, 338–351. https://doi.org/10.1016/j.jafrearsci.2018.06.032

Bhandari, A.K., Kumar, A., Singh, G.K., 2012. Feature Extraction using Normalized Difference Vegetation Index (NDVI): A Case Study of Jabalpur City. Procedia Technol. 6, 612–621. https://doi.org/10.1016/j.protcy.2012.10.074

Boori, M.S., Choudhary, K., Kupriyanov, A.V., 2020. Crop growth monitoring through sentinel and landsat data based ndvi time-series. Comput. Opt. 44, 409–419. https://doi.org/10.18287/2412-6179-CO-635

Bourenane, H., Bouhadad, Y., Tas, M., 2018. Liquefaction hazard mapping in the city of Boumerdès, Northern Algeria. Bull. Eng. Geol. Environ. 77, 1473–1489. https://doi.org/10.1007/s10064-017-1137-x

Chen, L., Li, M., Huang, F., Xu, S., 2013. Relationships of LST to NDBI and NDVI in Wuhan City based on Landsat ETM+ image. Proc. 2013 6th Int. Congr. Image Signal Process. CISP 2013 2, 840–845. https://doi.org/10.1109/CISP.2013.6745282

Chen, Y., Cao, R., Chen, J., Liu, L., Matsushita, B., 2021. A practical approach to reconstruct high-quality Landsat NDVI time-series data by gap filling and the Savitzky–Golay filter. ISPRS J. Photogramm. Remote Sens. 180, 174–190. https://doi.org/10.1016/j.isprsjprs.2021.08.015

Chouari, W., 2021. Wetland land cover change detection using multitemporal Landsat data: a case study of the Al-Asfar wetland, Kingdom of Saudi Arabia. Arab. J. Geosci. 14. https://doi.org/10.1007/s12517-021-06815-y

Choubin, B., Soleimani, F., Pirnia, A., Sajedi-Hosseini, F., Alilou, H., Rahmati, O., Melesse, A.M., Singh, V.P., Shahabi, H., 2019. Effects of drought on vegetative cover changes: Investigating spatiotemporal patterns, Extreme Hydrology and Climate Variability: Monitoring, Modelling, Adaptation and Mitigation. Elsevier Inc. https://doi.org/10.1016/B978-0-12-815998-9.00017-8

Deep, S., Saklani, A., 2014. Urban sprawl modeling using cellular automata. Egypt. J. Remote Sens. Sp. Sci. 17, 179–187. https://doi.org/10.1016/j.ejrs.2014.07.001

Demirel, H., Ozcinar, C., Anbarjafari, G., 2010. Satellite image contrast enhancement using discrete wavelet transform and singular value decomposition. IEEE Geosci. Remote Sens. Lett. 7, 333–337. https://doi.org/10.1109/LGRS.2009.2034873

EarthExplorer [WWW Document], n.d. URL https://earthexplorer.usgs.gov/ (accessed 4.16.23).

El-Asmar, H.M., Hereher, M.E., El Kafrawy, S.B., 2013. Surface area change detection of the Burullus Lagoon, North of the Nile Delta, Egypt, using water indices: A remote sensing approach. Egypt. J. Remote Sens. Sp. Sci. 16, 119–123. https://doi.org/10.1016/j.ejrs.2013.04.004

Fijani, E., Moghaddam, A.A., Tsai, F.T.C., Tayfur, G., 2017. Analysis and Assessment of Hydrochemical Characteristics of Maragheh-Bonab Plain Aquifer, Northwest of Iran. Water Resour. Manag. 31, 765–780. https://doi.org/10.1007/s11269-016-1390-y

Mehrnooshtahereezadeh@gmail.com

Fijani, E., Nadiri, A.A., Asghari Moghaddam, A., Tsai, F.T.C., Dixon, B., 2013. Optimization of drastic method by supervised committee machine artificial intelligence to assess groundwater vulnerability for maragheh-bonab plain aquifer, Iran. J. Hydrol. 503, 89–100. https://doi.org/10.1016/j.jhydrol.2013.08.038

Gandhi, G.M., Parthiban, S., Thummalu, N., Christy, A., 2015. Ndvi: Vegetation Change Detection Using Remote Sensing and Gis - A Case Study of Vellore District. Procedia Comput. Sci. 57, 1199–1210. https://doi.org/10.1016/j.procs.2015.07.415

Gao, B.C., 1996. NDWI—A normalized difference water index for remote sensing of vegetation liquid water from space. Remote Sens. Environ. 58, 257–266. https://doi.org/10.1016/S0034-4257(96)00067-3

Getnet, M., Amede, T., Tilahun, G., Legesse, G., Gumma, M.K., Abebe, H., Gashaw, T., Ketter, C., Akker, E. V., 2022. Water spreading weirs altering flood, nutrient distribution and crop productivity in upstream-downstream settings in dry lowlands of Afar, Ethiopia. Renew. Agric. Food Syst. 37, S17–S27. https://doi.org/10.1017/S1742170519000474

Gharebaghi, M., Sadatipour, S.M.T., Ghafourian, H., Agh, N., 2009. Quantitative and qualitative study of Kaveh Soda Factory's waste-water for growing of Artemia 4, 23–34.

Hamzehpour, N., Rahmati, M., 2017. Investigation of soil salinity to distinguish boundary line between saline and agricultural lands in Bonab Plain, southeast Urmia Lake, Iran. J. Appl. Sci. Environ. Manag. 20, 1037. https://doi.org/10.4314/jasem.v20i4.16

Han, S., Wang, B., Gutierrez, M., Shan, Y., Zhang, Y., 2021. Laboratory study on improvement of expansive soil by chemically induced calcium carbonate precipitation. Materials (Basel). 14, 1–23. https://doi.org/10.3390/ma14123372

Hu, Y., Dong, Y., Batunacun, 2018. An automatic approach for land-change detection and land updates based on integrated NDVI timing analysis and the CVAPS method with GEE support. ISPRS J. Photogramm. Remote Sens. 146, 347–359. https://doi.org/10.1016/j.isprsjprs.2018.10.008

Jaramillo, M.F., Restrepo, I., 2017. Wastewater reuse in agriculture: A review about its limitations and benefits. Sustain. 9. https://doi.org/10.3390/su9101734

Kathwas, A.K., Saur, R., Rathore, V.S., 2022. Impact of Flash Flood on Landuse and Landcover Dynamics and Erosional Pattern of Jiadhal River Basin, Assam, India. Smart Innov. Syst. Technol. 266, 389–396. https://doi.org/10.1007/978-981-16-6624-7_39/COVER

Khan, S., Ali, J., 2017. Chemical analysis of air and water, Bioassays: Advanced Methods and Applications. Elsevier Inc. https://doi.org/10.1016/B978-0-12-811861-0.00002-4

Kourgialas, N.N., Karatzas, G.P., Nikolaidis, N.P., 2012. Development of a thresholds approach for real-time flash flood prediction in complex geomorphological river basins. Hydrol. Process. 26, 1478–1494. https://doi.org/10.1002/hyp.8272

Lemenkova, P., 2016. Flow Direction and Length Determined by ArcGIS Spatial Analyst and Terrain Elevation Data Sets. Prior. Dir. Dev. young Res. farmers Mod. Sci. 579–583. https://doi.org/10.6084/m9.figshare.7210217

Long, D., Shen, Y., Sun, A., Hong, Y., Longuevergne, L., Yang, Y., Li, B., Chen, L., 2014. Drought and flood monitoring for a large karst plateau in Southwest China using extended GRACE data. Remote Sens. Environ. 155, 145–160. https://doi.org/10.1016/j.rse.2014.08.006

Lopes, C.L., Mendes, R., Caçador, I., Dias, J.M., 2019. Evaluation of long-term estuarine vegetation changes through Landsat imagery. Sci. Total Environ. 653, 512–522. https://doi.org/10.1016/j.scitotenv.2018.10.381

Mehrnooshtahereezadeh@gmail.com

673 Marchi, L., Borga, M., Preciso, E., Gaume, E., 2010. Characterisation of selected extreme flash
674 floods in Europe and implications for flood risk management. J. Hydrol. 394, 118–133.
675 https://doi.org/10.1016/j.jhydrol.2010.07.017
676 Masoud, M.H.Z., Basahi, J.M., Rajmohan, N., 2018. Impact of flash flood recharge on
677 groundwater quality and its suitability in the Wadi Baysh Basin, Western Saudi Arabia: an
678 integrated approach. Environ. Earth Sci. 77, 1–19. https://doi.org/10.1007/s12665-018-
679 7578-0
680 McFeeters, S.K., 2013. Using the normalized difference water index (ndwi) within a geographic
681 information system to detect swimming pools for mosquito abatement: A practical
682 approach. Remote Sens. 5, 3544–3561. https://doi.org/10.3390/rs5073544
683 Memon, A.A., Muhammad, S., Rahman, S., Haq, M., 2015. Flood monitoring and damage
684 assessment using water indices: A case study of Pakistan flood-2012. Egypt. J. Remote
685 Sens. Sp. Sci. 18, 99–106. https://doi.org/10.1016/j.ejrs.2015.03.003
686 Milanović, M., Tomić, M., Perović, V., Radovanović, M., Mukherjee, S., Jakšić, D., Petrović,
687 M., Radovanović, A., 2017. Land degradation analysis of mine-impacted zone of Kolubara
688 in Serbia. Environ. Earth Sci. 76. https://doi.org/10.1007/s12665-017-6896-y
689 Moharrami, M., Javanbakht, M., Attarchi, S., 2021. Automatic flood detection using sentinel-1
690 images on the google earth engine. Environ. Monit. Assess. 193, 1–17.
691 https://doi.org/10.1007/s10661-021-09037-7
692 Morar, C., Lukić, T., Valjarević, A., Niemets, L., Kostrikov, S., Sehida, K., Telebienieva, I.,
693 Kliuchko, L., Kobylin, P., Kravchenko, K., 2022. Spatiotemporal Analysis of Urban Green
694 Areas Using Change Detection: A Case Study of Kharkiv, Ukraine. Front. Environ. Sci. 10,
695 1–27. https://doi.org/10.3389/fenvs.2022.823129
696 Murray, N.J., Phinn, S.R., Clemens, R.S., Roelfsema, C.M., Fuller, R.A., 2012. Continental scale
697 mapping of tidal flats across east Asia using the landsat archive. Remote Sens. 4, 3417–
698 3426. https://doi.org/10.3390/rs4113417
699 Nageswara Rao, P.P., Shobha, S. V., Ramesh, K.S., Somashekhar, R.K., 2005. Satellite-based
700 assessment of agricultural drought in Karnataka State. J. Indian Soc. Remote Sens. 33, 429–
701 434. https://doi.org/10.1007/BF02990014
702 Narimani, V., Vafaee, B.S., Farokhzad, A., Chasemzadeh, R., 2011. Quantitative evaluation of
703 predominant of weeds in winter wheat and barley fields in Eastern Azerbaijan, Iran. Rev.
704 Científica UDO Agrícola, ISSN-e 1317-9152, Vol. 11, Nº. 1, 2011, págs. 126-133 11, 126–
705 133.
706 Nusrath, A., 2010. Vegetation Change Detection of Neka River in Iran by Using. J. Geog. 2, 58–
707 67.
708 Panigrahy S, Murthy T, Patel J, Singh T., 2012. Wetlands of India: inventory and assessment at
709 1: 50,000 scale using geospatial techniques. Current science:852-856
710 Pasley, H.R., Huber, I., Castellano, M.J., Archontoulis, S. V., 2020. Modeling Flood-Induced
711 Stress in Soybeans. Front. Plant Sci. 11, 1–13. https://doi.org/10.3389/fpls.2020.00062
712 Pires, H.R.A., Franco, A.C., Piedade, M.T.F., Scudeller, V.V., Kruijt, B., Ferreira, C.S., 2018.
713 Flood tolerance in two tree species that inhabit both the Amazonian floodplain and the dry
714 Cerrado savanna of Brazil. AoB Plants 10, 1–15. https://doi.org/10.1093/aobpla/ply065
715 Potter, C., 2021. Changes in the vegetation of New Orleans from the disturbance impacts of
716 Hurricane Katrina in 2005. Remote Sens. Appl. Soc. Environ. 24, 100611.
717 https://doi.org/10.1016/j.rsase.2021.100611
718 Pucciariello, C., Voesenek, L.A.C.J., Perata, P., Sasidharan, R., 2014. Plant responses to

Mehrnooshtahereezadeh@gmail.com

flooding. Front. Plant Sci. 5, 1–2. https://doi.org/10.3389/fpls.2014.00226
Ritter, J., Berenguer, M., Corral, C., Park, S., Sempere-Torres, D., 2020. ReAFFIRM: Real-time Assessment of Flash Flood Impacts – a Regional high-resolution Method. Environ. Int. 136, 105375. https://doi.org/10.1016/j.envint.2019.105375
Rouse J, Haas J, Schell J, Deering D., 1974. Monitoring vegetation systemsin the Great Plains witherts. In: Proceedings of the 3rd ERTS Symposium, Washington, DC, USA, vol 1.
Roy, P.S., Behera, M.D., Srivastav, S.K., 2017. Satellite Remote Sensing: Sensors, Applications and Techniques. Proc. Natl. Acad. Sci. India Sect. A - Phys. Sci. 87, 465–472. https://doi.org/10.1007/s40010-017-0428-8
Sajedi-Hosseini, F., Choubin, B., Solaimani, K., Cerdà, A., Kavian, A., 2018. Spatial prediction of soil erosion susceptibility using a fuzzy analytical network process: Application of the fuzzy decision making trial and evaluation laboratory approach. L. Degrad. Dev. 29, 3092–3103. https://doi.org/10.1002/ldr.3058
Saravanan, S., Jegankumar, R., Selvaraj, A., Jennifer, J., Parthasarathy, K.S.S., 2019. Utility of Landsat Data for Assessing Mangrove Degradation in Muthupet Lagoon, South India, Coastal Zone Management: Global Perspectives, Regional Processes, Local Issues. Elsevier Inc. https://doi.org/10.1016/B978-0-12-814350-6.00020-3
Shahbazi, F., Sahabnaghdi, I., Neyshabouri, M., Oustan, S., 2015. Assessing leaching of saline-sodic soils affected by Kaveh-Soda factory effluent using georeferenced maps in Maragheh-Bonab plain. Int. J. Adv. Sci. Eng. Inf. Technol. 5, 415–421. https://doi.org/10.18517/ijaseit.5.6.587
Shrestha, B.B., Kawasaki, A., Zin, W.W., 2021. Development of flood damage functions for agricultural crops and their applicability in regions of Asia. J. Hydrol. Reg. Stud. 36, 100872. https://doi.org/10.1016/j.ejrh.2021.100872
Statistical Center of Iran (2016) Retrieved from http://www.amar.org.ir.
Tucker, C., 1979. iw % SA Technical Memorandum 79620 Combinations for Monitoring Veqetation. Remote Sens. Environ. 8, 127–150.
Tucker, C.J., 1979. Red and photographic infrared linear combinations for monitoring vegetation. Remote Sens. Environ. 8, 127–150. https://doi.org/10.1016/0034-4257(79)90013-0
Valjarević, A., Filipović, D., Valjarević, D., Milanović, M., Milošević, S., Živić, N., Lukić, T., 2020. GIS and remote sensing techniques for the estimation of dew volume in the Republic of Serbia. Meteorol. Appl. 27, 1–14. https://doi.org/10.1002/met.1930
Verpoorter, C., Kutser, T., Tranvik, L., 2012. Automated mapping of water bodies using landsat multispectral data. Limnol. Oceanogr. Methods 10, 1037–1050. https://doi.org/10.4319/lom.2012.10.1037
Viana, C.M., Oliveira, S., Oliveira, S.C., Rocha, J., 2019. Land Use/Land Cover Change Detection and Urban Sprawl Analysis, Spatial Modeling in GIS and R for Earth and Environmental Sciences. Elsevier Inc. https://doi.org/10.1016/b978-0-12-815226-3.00029-6
Vrieling, A., De Leeuw, J., Said, M.Y., 2013. Length of growing period over africa: Variability and trends from 30 years of NDVI time series. Remote Sens. 5, 982–1000. https://doi.org/10.3390/rs5020982
Wahlstrom M, Guha-Sapir D., 2015. The Human Cost of Weather-Related Disasters 1995-2015. In. Geneva, Switzerland: UNISDR, CRED.
Wang, A., Wang, W., 2009. Superabsorbent Materials, Kirk-Othmer Encyclopedia of Chemical Technology. https://doi.org/10.1002/0471238961.supewang.a01

Mehrnooshtahereezadeh@gmail.com

765 Wang, Y., Li, Z., Tang, Z., Zeng, G., 2011. A GIS-Based Spatial Multi-Criteria Approach for
766 Flood Risk Assessment in the Dongting Lake Region, Hunan, Central China. Water Resour.
767 Manag. 25, 3465–3484. https://doi.org/10.1007/s11269-011-9866-2
768 Watson, E.R., Lapins, P., Barron, R.J.W., 1976. Effect of waterlogging on the growth, grain and
769 straw yield of wheat, barley and oats. Aust. J. Exp. Agric. 16, 114–122.
770 https://doi.org/10.1071/EA9760114
771 Weather data SYNOPS/BUFR - GFS/ECMWF forecast - Meteomanz.com [WWW Document],
772 n.d. URL http://www.meteomanz.com/index?l=1 (accessed 4.16.23).
773 World Meteorological Organization, 2015. Integrated Flood Management Tool Series | a.
774 Wu, Y., 2017. The Removal of Methyl Orange by Periphytic Biofilms. Periphyton 367–387.
775 https://doi.org/10.1016/b978-0-12-801077-8.00016-8
776 Xu, X., Zhang, Q., Tan, Z., Li, Y., Wang, X., 2015. Effects of water-table depth and soil
777 moisture on plant biomass, diversity, and distribution at a seasonally flooded wetland of
778 Poyang Lake, China. Chinese Geogr. Sci. 25, 739–756. https://doi.org/10.1007/s11769-015-
779 0774-x
780 Yariyan, P., Janizadeh, S., Van Phong, T., Nguyen, H.D., Costache, R., Van Le, H., Pham, B.T.,
781 Pradhan, B., Tiefenbacher, J.P., 2020. Improvement of Best First Decision Trees Using
782 Bagging and Dagging Ensembles for Flood Probability Mapping. Water Resour. Manag. 34,
783 3037–3053. https://doi.org/10.1007/s11269-020-02603-7
784 Youssef, A.M., Omer, A.A., Ibrahim, M.S., Ali, M.H., Cawlfield, J.D., 2011. Geotechnical
785 investigation of sewage wastewater disposal sites and use of GIS land use maps to assess
786 environmental hazards: Sohag, upper Egypt. Arab. J. Geosci. 4, 719–733.
787 https://doi.org/10.1007/s12517-009-0069-6
788 Zhang, X., Hu, Y., Zhuang, D., Qi, Y., Ma, X., 2009. NDVI spatial pattern and its differentiation
789 on the Mongolian Plateau. J. Geogr. Sci. 19, 403–415. https://doi.org/10.1007/s11442-009-
790 0403-7
791 Zhu, Z., Bi, J., Pan, Y., Ganguly, S., Anav, A., Xu, L., Samanta, A., Piao, S., Nemani, R.R.,
792 Myneni, R.B., 2013. Global data sets of vegetation leaf area index (LAI)3g and fraction of
793 photosynthetically active radiation (FPAR)3g derived from global inventory modeling and
794 mapping studies (GIMMS) normalized difference vegetation index (NDVI3G) for the
795 period 1981 to 2. Remote Sens. 5, 927–948. https://doi.org/10.3390/rs5020927
796
797